A Study on an Automatic System for Analyzing the Facial Beauty of Young Women

Neha Sultan

A Thesis

in

The Department

of

Computer Science and Software Engineering

Presented in Partial Fulfillment of the Requirements

For the Degree of Master of Computer Science at

Concordia University

Montreal, Quebec, Canada

January 2014

CONCORDIA UNIVERSITY

School of Graduate Studies

This is to certify that the thesis prepared

By: Neha Sultan

Entitled: A Study on an Automatic System for Analyzing the Facial Beauty of Young Women

and submitted in partial fulfillment of the requirements for the degree of

MASTER OF COMPUTER SCIENCE

complies with the regulations of the University and meets the accepted standards with respect to originality and quality.

Signed by the final Examining Committee:

_____ Chair
Dr. Jayakumar Rajagopalan

_____ Examiner
Dr. Tonis Kasvand

_____ Examiner
Dr. Yuhong Yan

_____ Thesis Supervisor
Dr. Ching Y. Suen

Approved by _____
Chair of Department or Graduate Program Director

_____
Dr. Christopher Trueman, Dean,
Faculty of Engineering and Computer Science

Date _____

ACKNOWLEDGEMENTS

My supervisor, Dr. Ching Y. Suen has provided me with constant guidance and invaluable feedback. I would also like to extend my gratitude to the Centre for Pattern Recognition and Machine Intelligence (CENPARMI) at Concordia University for providing the perfect environment for enabling innovation and excellence in research. I also thank the Natural Sciences and Engineering Research Council for the support associated with this research. In addition, the Faculty of Engineering and Computer Science at Concordia University has been a great source of invaluable knowledge and support for which I am grateful.

I would like to thank my family for always being there for me and for all their support.

DEDICATION

This thesis is dedicated to my parents, who encourage and support me constantly and due to their guidance I have been able to achieve my goals.

ABSTRACT

A Study on an Automatic System for Analyzing the Facial Beauty of Young Women

Neha Sultan

Beauty is one of the foremost ideas that define human personality. However, only recently has the concept of beauty been scientifically analyzed. This has mostly been due to extensive research done in the area of face recognition and image processing on identification and classification of human features as contributing to facial beauty. Current research aims at precisely and conclusively understanding how humans classify a given individual's face as beautiful. Due to the lack of published theoretical standards and ground truths for human facial beauty, this is often an ambiguous process. Current methods of analysis and classification of human facial beauty rely mainly on the geometric aspects of human facial beauty. The classifiers used in current research include the k-nearest neighbor algorithm, ridge regression, and basic principal component analysis.

In this research, various approaches related to the comprehension and analysis of human beauty are presented and the use of these theories is outlined. Each set of theories is translated into a feature model that is tested for classification. Selecting the best set of features that result in the most accurate model for the representation of the human face is a key challenge. This research introduces the combined use of three main groups of features for classification of female facial beauty, to be used with classification through support vector machines. The classifier utilized is Support Vector Machine (SVM) and the accuracy obtained through this classifier is 86%. Current research in the field has

produced algorithms with percentages of accuracy that are in the range of 75-85%. The approach used is one of analysis of the central tenets of beauty, the successive application of image processing techniques, and finally the usage of relevant machine learning methods to build an effective system for the automatic assessment of facial beauty. The ground truths used for verifying results are derived from ratings extracted from surveys conducted.

The proposed methodology involves a novel algorithm for the representation of facial beauty, which combines the use of geometric, textural, and shape based features for the analysis of facial beauty. This algorithm initially develops an overall landmark model of the entire human face. A significant advantage of this methodology is the accurate model of the human face which synthesizes the geometric, textural and shape-related aspects of the face. The landmark model is then used for extracting critical characteristics which are then used in a feature vector for training using machine learning. The features extracted help to represent facial characteristics in three major areas. Geometric features help to represent the symmetrical properties and ratio-based properties of landmarks on the face. Textural features extracted help capture information related to skin texture and composition. Finally, face shape and outline features help to categorize the overall shape of a given face, which helps to represent the given female face shape and outline for further analysis of any deviations from the basic face shapes. These features are then used in a classifier to appropriately categorize each image. The database used for the source of images contains images of female subjects from a variety of backgrounds and levels of attractiveness.

TABLE OF CONTENTS

LIST OF FIGURES

LIST OF TABLES

Chapter 1 Introduction

"Beauty is the shadow of God on the universe", said Gabriela Mistral, who lived on to become the first Latin American to win the Nobel Prize in Literature. People have often, though stereotypically, believed that what is good is beautiful. Due to the inherent tendencies of human beings, objects and creatures with features and appearances that are appealing to the eyes have traditionally been associated with positive responses and attributes. These and many more observations regarding the concept of beauty continue to intrigue and mystify humans. The aesthetic aspects of most animate and inanimate objects have been known to capture the undivided attention of great thinkers and scientists throughout history. It is indisputably human nature to ponder and marvel at the intricacies and beauty of people and objects surrounding us. Even more characteristic of humans is the tendency to focus on associated facial features and their indisputable connection with beauty.

The human face conveys extensive amounts of information; in essence, it speaks volumes about the individual it is associated with. Millions of dollars are spend on facial beautification and cosmetics; it has been shown that the amount of money spent on beauty related products in the US is more than the amount spent on education and social services [1]. Research has even conclusively shown that attractive faces activate centers of the brain that are associated with reward [2]. Studies have demonstrated that attractive people get preferential treatment and thus have greater tendencies towards achieving success. The socio-economic impact of facial beauty therefore helps stress the greater need for understanding of this basic concept. Significant amounts of research have been

conducted in the area of face analysis and recognition, a considerable portion of this research being in the area of facial beauty.

Science strives to explain the various phenomena of nature and hence it concurs naturally that the concept of beauty be approached and deciphered through the scientific method. This thesis attempts to describe and analyze extensively the concept of beauty from a technical perspective. It concentrates on building an automatic system for the measurement of female facial beauty. The approach used is one of analysis of the central tenets of beauty, the successive application image processing techniques, and finally the usage of relevant machine learning methods to build an effective system for the automatic assessment of facial beauty.

The ground truths used for verifying results are derived from ratings extracted from surveys conducted. Several key aspects and features that have been extensively shown to be associated with beauty will be discussed and then eventually utilized as features and main components. These features will then be used in a classifier to appropriately categorize each image.

1.1 Related Fields of Research

Research in the area of facial image processing has contributed to numerous successful studies. The human face itself has the potential to divulge great amounts of information that could prove to be of great use to researchers. The most commonly studied area is that of facial identity analysis. Additional areas include composite faces, human gender determination, age determination, and facial expression and emotional analysis. We will proceed to take a closer look at these related fields.

1.1.1 Facial Expressions and Emotions

Human facial expressions serve as an important component of communication between individuals. They are essentially based on movements of muscles beneath the skin of the face. Several studies in the area of machine learning have concluded in the creation of computational models of facial expressions. These models are of great use to scientists as facial expressions are of great importance in the fields of cognitive science, psychology, and neuroscience. Models of human emotion are also of great importance in the areas of artificial intelligence and human computer interaction systems.

Facial behaviors and expressions have numerous uses, which help aid in the daily communication aspects of individuals. Some primary aspects include:

- People often use expressions to depict what they are conveying, such as raised eyebrows for high pitches and lowered eyebrows for low pitches.
- Expressions are also used to control the flow of a conversation, for example people may gesture to let others know that they have finished talking.
- Human expressions often serve as signals of mental processes occurring, such as someone furrowing their brow when concentrating on a matter.

People also use expressions to consciously communicate their emotional states to other individuals.

There are two main models for representing human facial expressions. The categorical model assumes that there is a finite set of universal prevalent human expressions. These expressions can be divided into six main classes, which include joy, surprise, anger,

sadness, disgust, and fear [4]. This model is disputable because it assumes that facial expressions are universally innate, rather than dependent on culture. The continuous model, on the other hand, simply models each emotion as a feature vector, which each vector containing the various characteristics of each emotion.

By the categorical model, there are six main universal classified facial expressions which include joy, surprise, anger, sadness, disgust, and fear. The Facial Action Coding System helps to categorize facial expressions based on how they appear on an individual's face and which muscle systems are involved. This also allows any machine to systematically represent any facial expression in terms of constituent units called Action Units. Action Units are basically individual groups of muscles and their corresponding actions. There are approximately a hundred action units currently.

The main categories of Action Units are [5]:

- Main Action Unit Codes: these consist of basic facial muscle groups, such as “cheek raiser”, “brow lower”, etc
- Head Movement Codes: these describe the position of the head, such as “head turn left”, “head tilt right”, etc
- Eye Movement Codes: these describe where the eye is looking, such as “eyes turn right”, “eyes looking at another person”, etc
- Visibility Codes: these help to describe which parts of the face are not visible, such “brows and forehead not visible”, “lower face not visible”, etc

In order to classify facial expressions correctly, each facial expression is mapped to

several contributing action units and subsequently the facial images are analyzed for the presence of such facial action units.

The Automatic Face Analysis system was developed by Tian et al for the analysis of facial expressions based on the Facial Action Coding System. This system was trained and developed to recognize and analyze facial expressions based on two main features, which included permanent facial features and transient facial features. Table 1 illustrates the various action units and characteristics associated with each facial expression.

Facial Expression	**Number of Action Units**	**Description**
Anger	Four	Mouth and lips tightened, lowered and furrowed eyebrows, head facing straight ahead
Disgust	Three	Mouth open, upper lip raised, lower lip turned down, cheeks raised, protruding lips
Fear	Six	Mouth open slightly, eyebrows raised, perspiration, eyes wide open
Happiness	Two	Eyes wide open, mouth corners raised and lowered, mouth pulled back at the corners, skin under eyes has wrinkles
Sadness	Three	Mouth corners depressed and lowered, inner portion of eyebrows raised
Surprise	Four	Arched eyebrows, eyes opened widely to expose more white portion of eye, lips protruded, jaw slightly dropped

Table 1: Descriptions of Main Facial Expressions

1.1.2 Composite Faces

Sir Francis Galton has long been known famously as one of the pioneers in the areas of composite imaging, a lot of what is known about his methodology comes from his

extensive documentation called “Composite Portraits”, which was published in London in 1878. The process essentially involved superimposing multiple exposures of various individuals' faces on a single photographic plate. An inherently observant scientist, Sir Galton, also hypothesized that these composite portraits would be more attractive than the individuals used to create them. This has been known to be the basis of research in the 1900s on the influence of “averageness” on facial attractiveness[6]. Going further, Sir Galton further proposed that these composite faces could also represent various human ideals, concepts, and even various categories and characteristics of people. Concluding from this, he began modeling composite faces that would represent features that were commonly found in various types of humans, such as murderers, doctors, etc.

Significant changes have been made in this field, with major improvements in terms of speed, accessibility and automation. Research has been done in automatic extraction and blending of human faces into media content.

Another aspect of composite faces is one in which the picture is made up of two halves, one half from one person and the other from another person, thus coming up with a new image. Considerable studies have been done on the effects of these images. The human brain can oftentimes effortlessly distinguish a face from the various other image patterns available. Moreover, it does not require much effort to distinguish one face form another as well. However, in the case of composite faces made up of two different humans, the brain often faces an optical illusion [8].

When the same top half of a facial image is paired with various different bottom halves of a facial image, the observer is often led to believe that the identical top halves might be

non-identical. This illusion, known as the composite face illusion, still occurs when the viewer consciously knows that the top halves are in fact identical.

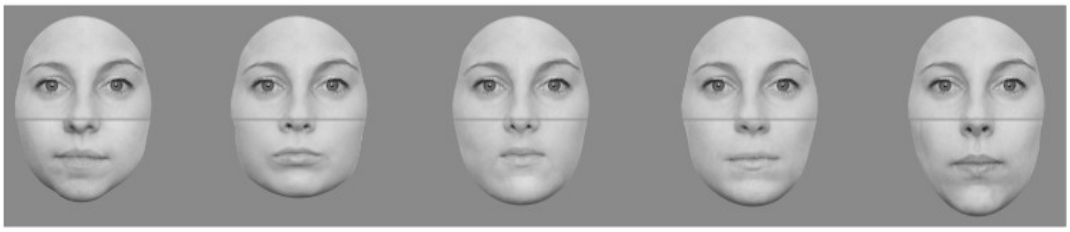

Figure 1: Illustration of the composite face illusion. Here the top halves of the images are all identical, and they are paired with different bottom halves of images. This gives the illusion that the top halves of the images are also different.

Composite faces have also been used to theoretically model "average" faces for women of different nationalities and ethnicities. It has often been observed that these composite faces are more attractive than the faces used to produce them. This has been hypothesized to be due to the fact that in the process of calculating the composite images, any irregularities and asymmetries present in the component faces become neutralized. The skin on the resulting composite face looks very young and smooth, because any facial marks such as pimples and wrinkles also disappear during the blending process.

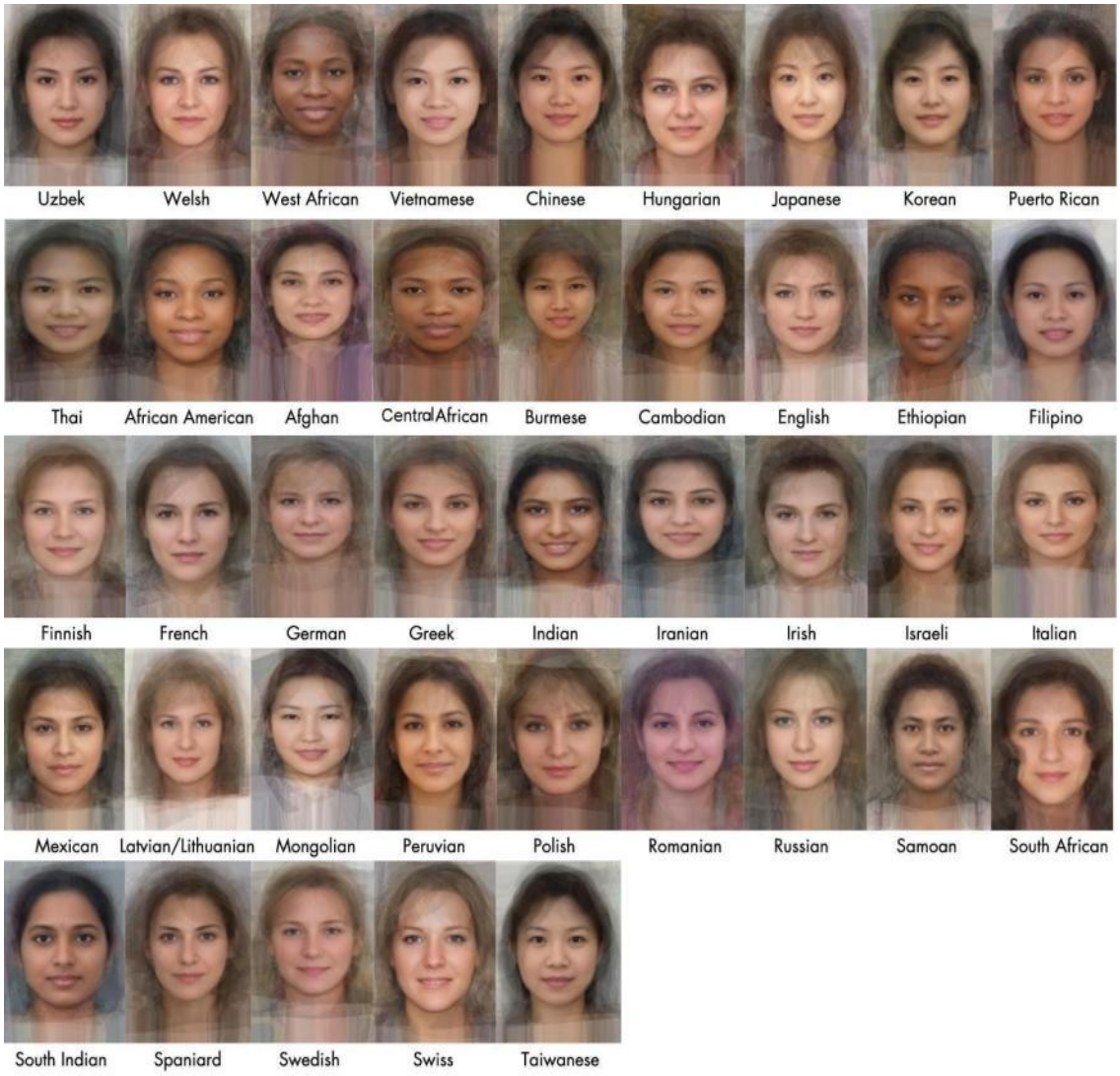

Figure 2: Composite faces representing various nationalities [9]

1.1.3 Gender Classification

Given a facial image, human gender analysis and classification mainly aims to determine through select methods whether the image belongs to a male or female human. Gender identification has several applications and benefits. It even has the potential to help considerably in the field of facial recognition. Identification of the gender as a

preprocessing step for facial identification would technically make the process twice as fast as it would initially classify the image set into two halves, one for the female participants and one for the male. Gender classification is often important for the development of human computer interaction systems that are able to evolve and customize the experience of the user according to gender.

Currently many retail operations and are attempting to customize their general customer experience by identifying the specific gender of the people passing by their outlets. This eventually helps to target advertisement towards the specific related gender and in turn increases revenue for the outlets. Several more important uses for gender identification and analysis are as below:

- demographic data collection
- human computer monitoring
- robotics applications
- psychotherapy applications
- surveillance and security
- biometrics

Two main approaches to the problem of gender classification include feature based and appearance based models [10]. In the feature based model, various features are extracted from the image and the overall gender detection process is based on the analysis of those features. Some examples of features commonly used include features extracted from the geometry of the face, edge information, and even skin color information. The appearance based model, on the other hand, basically aims to input the entire image as the basis of analysis rather individual features of the image.

Several novel methods have been developed over the years in the area of gender classification. Baluja and Rowley [11] used the Adaboost classifier, which helped them achieve over ninety-three percent classification. This was higher than the accuracy that they received with support vector machines, for which the input used pixels. The Adaboost classifier also had considerable increases in speed, achieving fifty times faster classifications than support vector machines.

1.1.4 Facial Beauty Analysis

Considerable research has been conducted in the areas of image processing and machine learning. A certain portion of that has focused on aspects related to the human face. A very integral aspect of the human face is its own characteristic natural beauty; beauty that has inspired, motivated, and generated a considerable extent of debate and discussion. The idea of quantifying beauty has been approached and extensively studied throughout the ages. Therefore, various methodologies and theories have been proposed by several leading scientists in the disciplines of image processing and machine learning. The approach has varied greatly, with some focusing on aspects of measuring beauty through human raters, some preferring to quantify beauty through regression techniques, while others assessed the effects of certain factors on the perception of beauty. This section presents the various scientific approaches to the analysis of human facial beauty.

Perett et al [23] examined the role of symmetry in the perception of beauty for a given face. Several experiments were conducted to help determine the role and contribution of symmetry. All experiments involved presenting a group of raters with a set of images to rate according to their preferences. The first experiment involved making three

symmetric versions of a given facial image. The versions included a symmetric remapping, a left-mirrored image, and a right-mirrored image. The results of this first experiment noted that more of the raters preferred the images with enhanced symmetry. Also, the results were also influenced by the gender of the rater and the raters were not aware that a certain portion of the images had been edited to enhance symmetry.

Figure 3: Images with no enhanced symmetry (left) and an image with enhanced symmetry (right)

The second experiment aimed to observe the role of symmetry in the absence of textural asymmetries. Therefore, pairs of images were used, with the comparison being made between the normal image and a blended symmetric composite image. The results of this experiment also showed a strong preference for the symmetric version of the image. Thus, the overall results of the experiments provided strong evidence for the influence of facial symmetry towards facial attractiveness. Figure 3 shows the pair of images being compared with the left image being the normal image and the right image being the symmetric composite image. Figure 4 shows the relative distributions of symmetry in the raters that participated in the various experiments conducted.

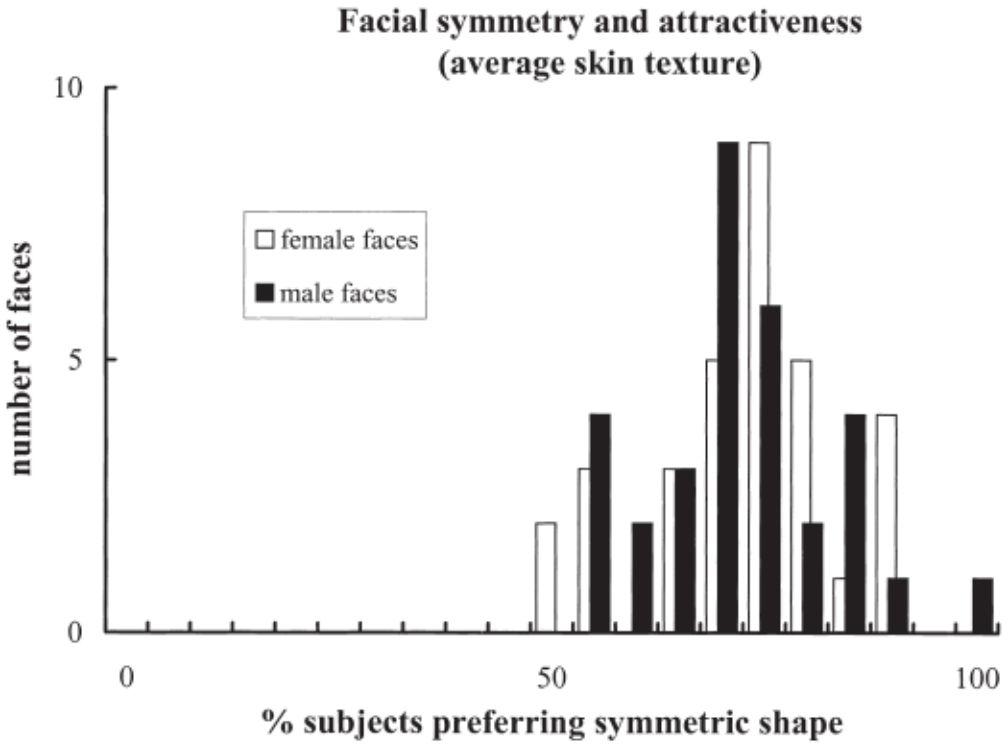

Figure 4: Distribution of respondents preferring symmetry

Other research has focused on various approaches to using image processing and machine learning techniques for the analysis of facial beauty. Davis and Lazebnik examined the facial attractiveness using manifold kernel regression. The images were obtained from a website that also provided attractiveness ratings that various raters had assigned to each image. Subsequently, a regression estimator was defined that returned an image in terms of its given attractiveness value and kernel bandwidth. Then, the geometric change for each image with the attractiveness score taken into consideration is calculated. Finally, this result is analyzed to determine facial patterns as a function of attractiveness.

Another approach to the analysis of facial beauty was proposed by Aarabi et al [3]. The research aimed to automatically score the beauty of a given image based on various ratios

between facial features. The methodology involved first isolating the various facial features, which is done in three major steps that include face localization, left and right eye localization and mouth localization. In addition, a set of images is rated by human raters. These ratings are then collected and a K-nearest neighbor algorithm is applied in order to generate a beauty assignment function. This function essentially is tasked with the predicting the beauty score for a given image.

1.2 Problem Description

Beauty is a central aspect of human psychology and social interactions; thus a considerable amount of thought and research has been conducted in its related fields. The ultimate question eventually results in being one that relates to understanding exactly what it is that makes a face beautiful. Undoubtedly, beauty is easy to identify but rather difficult to quantify. Some studies have shown that faces based on average face blends are associated with high attractiveness ratings, whereas others claim that images with a certain variance from the mean produce higher ratings.

Analysis of human facial beauty is a much researched field in the area of image processing and machine learning. Numerous contemporary studies exist which assist in the understanding of what constitutes beauty. Cunningham conducted experiments which helped to determine which particular features of females elicited responses of attraction from males [12]. Furthermore, Wu et al analyzed the aspect of cross-cultural perceptions of female physical attractiveness, in an effort to basically analyze the consistency of attractiveness ratings and characteristics across various cultural groups [13].

In addition, research has effectively delved into the topic of computational analysis of

facial beauty, which remains one of the most important aspects of beauty analysis. Schmidhuber attempted to automate the creation of an ideal face through fractal geometry [14]. Moreover, it has been shown that beauty has several aspects to it, which include symmetry, texture, and geometric ratios. It is only when all these aspects are taken into consideration that beauty analysis results are more accurate. This thesis attempts to address this need and also incorporate further techniques to improve the results obtained.

1.3 Main Contributions

This thesis focuses on the development of an automatic beauty analysis system. It aims to be able to classify the attractiveness levels of a given image of a female subject. Several theories exist regarding the evaluation of esthetic facial beauty and these are compared with the ratings from human survey participants. This is of paramount importance as it helps to validate the accuracy of the beauty assessment result so that it is based on actual human observations and thus is not limited only to image analysis. The main contributions include:

(a) **Application of several key feature vectors to form an accurate representation of beauty for a given face:** Geometric features, edge histograms, and texture analysis have been incorporated for the analysis of beauty of a given image. This is a novel approach as until now the aspect of texture has not been utilized much in research. Moreover, the combination of these three aspects has not been studied much in detail in previous research.

(b) **Large population size with ratings as ground truth:** There is an imperative need to validate the presence of beauty through accurate standards and ground

truths. Since, this study essentially aims to predict and analyze the presence of beauty as it would be perceived by a human, the ground truths have been chosen to be a set of ratings submitted by an eclectic group of survey participants. This method has been used previously; however the number of images used are greater in this research. The amount used in previous research ranges between 40 to 90 images. This research makes use of 215 images.

(c) **Feature detection and extraction using Active Shape Models:** The method used to extract the geometric features involved detecting certain key regions on the faces, making it imperative that the process that is used to locate them resulted in very accurate results. The approach of active shape models was thus used to precisely pinpoint each key landmark on the face, this procedure greatly increased the accuracy with which key feature positions were determined.

(d) **Texture Analysis and Edge Contour Information:** The texture components of a given image were analyzed to account for the various facial textures possible that are present in human faces. In addition, the characteristics corresponding to various face shapes were extracted using edge contour information. This helped to take into consideration both face texture and facial shape, which are key aspects of the aesthetics of any given human face.

(e) **Support Vector Machines:** The major classifiers used in beauty analysis research lately include K-Nearest neighbor classifier, linear discriminant classifier, and decision trees. The use of support vector machines has been limited. This thesis aims to use support vector machines as a means to provide

higher accuracy by using it as the main classifier.

1.4 Applications of Automatic Beauty Analysis

The automatic analysis of human facial beauty has numerous potential applications in our daily life. A large portion of cosmetic surgery is concerned with the improvement or beautification of facial regions. This program can help aid the surgeon as a predicting tool to guide the surgeon and decide what corrections need to be made in order to achieve ideal beauty assessment results. A key result of this will be that the surgeon's decisions will no longer be based on subjective assessments; rather they will be validated by this tool.

This tool can also be used for the development of recommended systems that are capable of making human-like judgments based on aesthetic aspects of human faces, essentially making use of computer-vision to replace human assessment of facial beauty. In addition, this tool also has significant uses in improving the understanding of the human psychology behind the concept of beauty by helping to determine and scrutinize the reasoning behind it.

Furthermore, there is a large scope for the application of this tool in the cosmetics industry, mainly in the facial enhancement industries such as those manufacturing products such as concealers, foundation, eye shadow, lip products, etc. By providing validation of the beauty enhancing power of these products, this tool will be able to generate more concrete standards in the cosmetic makeup industry and hence provide certain benchmarks for assessment of their benefits.

Chapter 2 Standards and Theories Associated with Facial Beauty

Beauty is defined as the blend of qualities that provides pleasure to the senses, in particular the sense of sight; these qualities are often attributes associated with the shape, color, and form of an object. In another associated definition, beauty can be described as the combination of qualities that are pleasing to the intellectual or moral senses as well. As another example of the various definitions of beauty, general thought throughout the Middle Ages believed that beauty was an integral component of the cosmos that was often associated with harmony, order, and mathematics.

2.1 Beauty Throughout the Ages

Classical philosophy, another major influence in ancient thought, depicted beauty as one of the main intrinsic supreme values that were a core component of the beliefs of that time, being revered as much as truth, goodness, love, and the divine. Thus, the perception of beauty of ancient philosophy was mainly centered on the concept of beauty being a timeless ideal.

The Ancient Greeks were inarguably one of the largest contributors to classical philosophy. The word beauty is derived and etymologically related to the words "kalos" and "horais", where "horais" essentially was related to the word "hours". This provides us with an interesting perspective on the Ancient Greek's views of beauty, meaning that beauty was associated with a particular individual projecting himself correctly within the time frame of his age. Fundamentally, this can be analysed as the Greeks subtly referring to the view that people appearing in sync with their age were considered beautiful, it was akin to females and males not trying to appear too young or too old. Moderation,

symmetry and proportion formed the basis of the Ancient Greeks' perception of all that was beautiful. It is believed that such a perspective was not significantly skewed from the modern day viewpoints of objects of aesthetic nature [24].

In Ancient Greek society, beauty was not limited to just the appearance but was also found in objects that provided pleasure in a wide range of sense. In addition, beauty was associated with noble birth, right conduct, social status, and general usefulness, demonstrating that the ancient Greeks did not merely associate beauty with ephemeral outward appearances. "Kalokagatia", which meant "beauty-good “in ancient Greek, described the presence of beauty in inherently "good" things. This was a commonly used expression, illustrating the deep connection that Greeks felt between beauty and the general 'goodness' present in an object [25].

The Greeks were concerned with the essence of beauty and how beauty contributes to the ultimate "good", as understanding what is good and what contributes to the ultimate happiness constituted one of the many pillars of Greek philosophy. Beauty was also studied with respect to other virtues such as truth and goodness.

2.1.1 Pythagoras's Contributions

Pythagoras, a famous Greek philosopher and mathematician, was greatly interested in the natural processes of the formation of world as well the basic essence of existing human beings. However, his approach sought to explain why and how the world was structured and maintained its harmony. Pythagoras believed that mathematics unites the universe and it in turn imparts order and rhythm to the world. This order helps to maintain a balance in the cosmos as well as in the souls of beings. He firmly believed that harmony

in the universe is built upon mathematical order and that beauty was the main objective principle that maintains this harmony. Thus, he proposed the theory that aesthetic experiences are closely associated to and based upon mathematical ratios related to tones and rhythms [26].

2.1.2 The Golden Ratio

The discovery of the Golden Ratio is mainly attributed to Pythagoras. This ratio has fascinated many intellectuals and philosophers alike for more than 2500 years. The golden ratio is essentially the ratio between any two quantities, a and b, such that the ratio of the two is equal to the ratio of their sum to the maximum of the two. This ratio is represented by the Greek letter phi, φ. It is illustrated below:

$$\frac{a+b}{a} = \frac{a}{b} = \varphi.$$

In order to calculate the value of φ, we must start with the left fraction and simplify it by substituting in b/a with 1/ φ. This is shown below:

$$\frac{a+b}{a} = 1 + \frac{b}{a} = 1 + \frac{1}{\varphi}$$

We then have:

$$1 + \frac{1}{\varphi} = \varphi$$

The next step involves multiplying with φ to further simply the expression to:

$$\varphi + 1 = \varphi^2$$

This expression is rearranged so that we now have:

$$\varphi^2 - \varphi - 1 = 0$$

The use of the quadratic formula allows us to solve this equation and we obtain a positive solution as below:

$$\varphi = \frac{1+\sqrt{5}}{2} = 1.6180339...$$

Therefore, the Golden Ratio has an ideal value that is approximated by 1.618. Pythagoras discovered that the Golden Ratio was often present in creations of beauty. He noticed that music that was pleasing to the ears had notes and beats that occurred at intervals corresponding to the Golden Ratio. Furthermore, he also noticed that several naturally occurring organisms followed the Golden Ratio, such as in seashells, flowers and even in the human body. It was even observed that the arrangements of petals in a flower occurred at degree intervals that followed the Golden Ratio. In the 1200s, one of the most prevalent patterns in nature, the Fibonacci sequence, was also found to follow the Golden Ratio [29].

In the years to follow, Leonardo da Vinci published a dissertation that discussed ideal design proportions based on the Golden Ratio. The famous Vitruvian Man, developed by da Vinci, also followed proportions based on this ratio. Various architectures and monuments throughout the years have been found to follow the Golden Ratio, although it is not evident whether the architects had this ratio in mind during construction. The Parthenon and the Pyramids of Giza consist of architecture that abides by the ratio.

Of evident interest is the presence of this ratio in humans, and this ratio has indeed been observed in the various aspects of the human form. As an example, the lengths of the

fingers of the hand have in fact been observed to be larger than the preceding one roughly by the Golden Ratio. Leonardo da Vinci has already described the ideal proportions and measurements for the human body through the Virtuvian Man. In addition to this, the Golden Ratio has been observed in the very arrangement of the features of the human face. The positions of the mouth and nose are such that they each lie at the golden sections of the distance between the eyes and the chin. It has often been observed in people that are perceived to be attractive that the ratios and proportions of the face closely follow the Golden Ratio. Furthermore, it has been theorized that adherence to the Golden Ratio is a possible indication of good health and fitness [29].

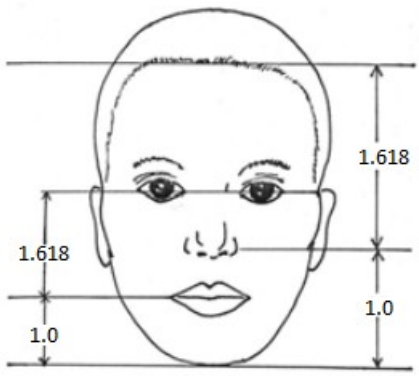

Figure 5: Representation of Golden Ratio on a Human Face

2.1.3 Plato

Plato has been known as one of the most famous philosophers and mathematicians of ancient Greece and has contributed to some of the most well documented dialogues in philosophy. Plato perceived virtues such as "beauty", "good" and "justice" as divine entities. Believing that beauty was not related to any psychological aspects of the mind,

Plato stressed that it was instead an existing and eternal being of a divine nature. Beauty was believed to exist in perfection in the form of Gods and an imperfect form while on Earth.

Plato also sought to explain how human beings become familiar with the concept of beauty, thus providing an explanation for how humans understood the concept. He theorized that every human is born with an inherent understanding of beauty, and that individuals seek to develop this concept throughout their lifetime [29].

2.1.4 Aristotle

In contrast to the beliefs of Plato, Aristotle perceived beauty as a property of nature itself and not as a permanent divine being. Aristotle did believe that beauty and 'goodness' were related, however he made clear distinctions between the two concepts.

2.2 Modern Philosophy

Rather than focusing on the metaphysical aspects of objects as done in classical philosophy, modern philosophy has shifted the focus towards the human senses. In the 1700s, Alexander Baumgarten coined the term "aesthetics", which was defined as the study of human sensibility. This was a turning point in the study of perception of beauty, as the focus was no longer on the metaphysical and ontological associations of beauty. Beauty no longer was approached in the same manner as love, truth, goodness and other virtues. It was Immanuel Kant, who formally established the study of beauty as a separate discipline, with the study focusing mainly on the concept of beauty, the values associated with it, and the related expressions of beauty in art.

There are several key aspects that differentiate the modern approach to the study of beauty and the classical approach:

- there is more weight given to the views and contributions of the observer with regard to the judgment of beauty
- there is not much emphasis on the concept of moral beauty
- the concept of mathematics with relation to beauty is not considered, in addition to the scientific nature of beauty

In modern philosophy, it is often argued that there needs to be greater emphasis on the individual's judgment of beauty as the interaction between a subject and a given object. Philosophers admit that the segregation of the notions of beauty from morals and virtues have had a diminishing effect on the modern conscience and attitude towards the concept of beauty [30].

2.3 Evolution and Beauty

Attractiveness is an integral component of the overall personality of an individual. In the interaction between two individuals, there occur natural attempts on both sides to analyse and incorporate the information perceived about the other in order to formulate a model. This model is then used to understand the motives and even predict the other person's actions. Therefore, attractiveness plays a large part in deciding the nature of social interaction that may occur between two individuals.

Researchers have observed that attractiveness preferences are very closely related to evolutionary theory. How humans perceive and in turn interpret facial features has been theorized to be depended upon inherent factors based on natural selection. This

essentially means that human judgments of attractiveness are not based on mere whim, but instead reflect years of evolutionary fine-tuning. These judgments reflect an assessment of mating potential and quality. Attractive faces are seen as indications of a healthy and parasite-free body, in addition to social competence, intellectual capability, and psychological adaptation [31].

With this in mind, it is important to point out which particular features help to reflect these evolutionarily favorable characteristics. Research has observed that mainly features that are typically characteristic of a gender are often integral in determining attractiveness. There features include a small chin, full lips, high cheekbones, narrow nose, and an overall small face. These are characteristics that are considered very 'female' and thus may indicate youth and fertility, which in turn cause them to be considered attractive [31].

2.4 Objectivity of Facial Beauty

There are several questions that arise when considering the concept of beauty. The main question that often occurs is: "What are the exact characteristics and features that make a face 'beautiful'?" An equally often asked question is: “Do there exist universally accepted standards of beauty?" This research aims to automate the analysis of facial beauty. In order to do so, we must hypothesize that beauty has cross cultural standards.

There has been extensive research and evidence helping to demonstrate that beauty is universal and even hard-wired in humans. This helps to show that humans perceive beauty cross-culturally, cross-racially, and irrespective of age-groups [32]. The cross-cultural consistency of beauty has often been established through brain activity patterns

in humans, studies of infant preferences, as well as beauty ratings from surveys.

Brain activity patterns have been studied to understand the response that the human brain undergoes when processing an attractive face. Scientists in the areas of neurophysiology have detected areas of the brain that process the assessment of facial beauty. In addition, major activity patterns that relate to specific judgments of attractiveness have been measured. These patterns have shown a strong correlation with beauty scores and hence help to establish the objectivity of beauty [33].

By studying preferences and responses of young babies, scientists have been able to understand the objectivity of human beauty. Babies around the age of three to six months were given sets of images to look at and the time spent by each baby looking at the images was monitored. The images had attractiveness ratings provided by adult raters. An analysis of the data showed that the babies were able to distinguish between attractive or unattractive faces. Since babies are not necessarily affected by cross-cultural paradigms, this helps to indicate that appreciation of beauty is a cross-cultural and inherent human characteristic [34].

Furthermore, several experimental surveys have been conducted in order to collect attractiveness ratings. These surveys usually involve a group of raters rating a large set of images of diverse individuals. A consistency in ratings is observed when there is a correlation greater than 0.9. It has been observed that there is a consistency in ratings between groups of Hispanic, Black, Asian, and White Americans. This consistency is also presented between male and female respondents. It was thus concluded that there is a consistency in the perceptions of beauty in various ethnicities, genders, and age groups.

2.5 Theories Related to Facial Beauty

In order to analyse and automate the prediction of facial beauty, there need to exist certain characteristics and theories which we can associate beauty with. This research aims to quantify beauty through mathematics. Several aspects have been shown to predict attraction to a particular face. The various factors include:

- prominence of facial features
- facial skin texture
- positions of facial features
- relative luminous intensity of facial features

A brief overview of the major theories behind the assessment of facial beauty is further presented in the following.

2.5.1 Averageness

Several studies have been conducted in the area of composite faces. Composite faces are essentially formed from sets of faces combined together; research has found that a composite face is perceived to be more attractive than the various components that form the particular face. Moreover, there is an increase in the attractiveness ratings as more faces are added to a composite face [35].

Alteration of a face such that its composition is similar to the average of a set of faces has been found to enhance beauty, and altering the composition away from the mean tends to decrease the perceived beauty.

2.5.2 Symmetry

Facial symmetry has traditionally been one of the main assessments of facial beauty. Symmetry has been shown to be a benchmark for the ultimate beauty and has significant affect in attractiveness ratings for females in particular [36]. The human fetus is designed to develop in two equal parts around the central axis of the spine. However, this process is not always perfect; genetic abnormalities, poor nutrition, and infections can modify the facial design leading to asymmetries.

Facial symmetry is also believed to be an indication of good health and fitness, in addition to being a good sign of developmental stability [37]. The ideal face would literally consist of the two halves being identical when superimposed, with the eyes lining up evenly, the smile being straight and the nose, cheeks and forehead being perfectly balanced. Symmetry has been associated with elegance, poise, tidiness, and more importantly genuine femininity [38].

2.5.3 Skin Texture

The skin is the largest organ in the human body and is also the body's first layer of defense against harmful substances. Over time and as the body ages, skin tends to sag and lose vital nutrients and fats. In addition to this, pollution, prolonged sun exposure, and very dry climate can have adverse effects on skin texture. Good care, exfoliation, and moisturization are key factors for maintaining healthy skin. This is integral as skin appearance has a significant impact on the overall perceived beauty of an individual.

A woman's facial skin texture greatly influences the attractiveness ratings. The ideal skin

has a balanced distribution of skin color which is evenly spread throughout. In addition, the skin surface's topography is also evenly distributed. It has been found that skin texture plays a critical role in the high attractiveness ratings of averaged composite faces. This is because any imperfections such as wrinkles or acne are eliminated in the averaging process, resulting in a composite face with relatively smooth skin texture [39].

2.5.4 Geometric Facial Features

Attractiveness can also be measured using facial cues and landmarks. In this procedure, various facial features, such as the corners of the eyelids for example, are used as reference points. Consequently, geometric features are measured and distances are calculated. Therefore, an overall facial representation is developed through the calculation of a set of geometric features [40]. The representation obtained contains the set of facial features, such as the eyebrows, eyes, nose, and mouth, in addition to the facial outline.

2.5.5 Golden Ratio

The Golden Ratio is the relationship that exists between any two quantities, x and y, when their ratio is equivalent to the ratio of their sum, (x + y), and their maximum. The value of the Golden Ratio itself is approximately equal to the ratio of 1.618 to 1. The Golden Ratio theory is based on the idea that beauty in objects is associated with and perhaps due to certain inherent ratios and proportions which lead to the exhibition of aesthetic qualities. The Golden Ratio theory asserts that the ideal face is such that has the major facial proportions fitting the Golden Ratio. There are various ratios and

measurements associated with the human face; ideal facial beauty exists when these measurements correspond to the Golden Ratio [43].

2.5.6 Facial Thirds

The human face ideally can be divided into equal thirds by drawing horizontal lines going through the forehead hairline, the eyebrows, the tip of the nose and the base of the chin. The upper third covers a region extending from the hairline to a line going through the top of the eyebrows, the middle third's region extends from the top of the eyebrows to a line going through the tip of the nose, and the lower third covers the region from the tip of the nose until the chin [45].

In the ideal facial beauty these regions would be roughly equal. Beauty analysis is then made based on measurements that help validate the existence of these thirds and furthermore assess how equal they are in terms of size.

Chapter 3 Data Analysis and Collection

Several large databases are available for conducting studies in image processing and machine learning. Databases form an integral component of research in these areas, as they help to test the accuracy of any given algorithm against standard available data sets. As there are various forms of research being done in image processing, various kinds of databases have been developed and maintained over the years to help assist the particular kind of research. There is a very strong correlation between the success of an image processing application and the availability of a database with data related to the application. Databases are often developed so that they can be suited to a wide variety of applications. In order to do so, such databases contain large variations of the images associated as well as a large amount of meta-data to help establish ground truth and provide additional data related to the images present in the database.

On the other hand, there also exist databases that are solely developed for particular aspects of research. Thus, they are only suitable for certain applications and contain custom data to enable the extraction of features related to the specific research being done. Furthermore, a large portion of facial image databases was initially developed solely for the purpose of testing face identification models and thus contain mostly gray scale images. In recent times, there has been an increase in the number of databases containing colored images.

Some widely used image processing databases include:

1. **PIE Database**

   - developed at Carnegie Mellon University, Pittsburgh, Pennsylvania, United States

   - contains 41368 images

   - 68 subjects

   - 13 different poses

   - 43 different illumination conditions [15]

2. **Yale Face Database**

   - developed at Yale University, New Haven, Connecticut, United States

   - contains 165 images

   - 10 subjects

   - 11 different expressions

3. **FERET Database**

   - developed at George Mason University, Virginia, United States

   - 14126 images

   - 1199 subjects [17]

4. **MIT-CBCL Face Recognition Database**

   - developed at Massachusetts Institute of Technology, Massachusetts, United States

   - more than 3000 images

   - 10 subjects [18]

5. **Face Recognition Data**

   - developed at University of Essex, England

   - 7900 images

   - 395 subjects

   - 20 different images per individual [19]

6. **M2VTSDB Database**

   developed at University of Surrey, England

   - 333 images

   - 37 subjects

   - 5 different images per individual [20]

7. **AR Face Database**

   - developed at Purdue University, Indiana, United States

   - 4,000 images

   - 126 subjects [21]

8. **BioID Face Database**

   - developed by HumanScan AG, Switzerland

   - 1521 images

   - 23 subjects [22]

9. **CalTech Faces Database**
   - developed by the Computational Vision Department at California Institute of Technology, California, United States
   - 450 images
   - 27 subjects [23]

The above is just a brief description of the various databases commonly used in image processing research, not all of the databases mentioned were utilized for the purposes of this research. The section below gives an overview of the databases that were used in this research.

3.1 Databases Utilized in this Research

This research aims to develop a tool for automatically analyzing the facial beauty in a given image. In order to do so, as previously discussed, we have made the assumption that beauty is viewed in a similar aspect across cultures. In order to remain consistent with this assumption, this project utilizes images from databases containing images of individuals from different ethnic backgrounds. Images from a total of five main databases have been used for this research. The ethnicities incorporated in this research include American, Latin-American, Asian, and European. The images for European individuals include data taken from two databases, one containing images of British individuals and another containing images of Dutch individuals. The Asian ethnicity was represented through images from Chinese and Indian individuals. The following is a detailed description of the images utilized for this research.

Normalization is an imperative step in the process of image processing, as it essentially

establishes consistency in the input images, hence being a critical component of ensuring the validity and accuracy of results being obtained. Standardized and well processed images also help improve the likelihood of success for any suggested approach.

The main focus in this research has remained on the analysis of human facial beauty in females, therefore all the images utilized in this research are of females. It was necessary to pre-process and normalize the images prior to their usage as inputs. Several steps were necessary to ensure that all the images resulted in the same range of pixel intensity and range of grayscale. The images were all resized and formatted to the dimensions of 800 pixels in height by 720 pixels in width and further converted to grayscale.

Some of the images in various databases had the subject wearing glasses or other facial ornamentation. Such images were not used as the research focuses on images of females with no facial ornamentation or device. All the subjects are also seen as having a forward facing pose with a neutral expression. Furthermore, the subject's photo contains the head, neck, and the top portion of the shoulders.

3.1.1 AR Face Database

The AR Face Database was compiled at Purdue University in the year 1998 by Aleix Martinez and Robert Benavente. It was a joint collaboration by the two researchers from different universities. Robert Benavente was studying at the Computer Vision Centre Universitat Autonoma de Barcelona, while Aleix Martinex was studying at the Robot Vision Lab at Purdue University. It is essentially a freely available public database which was intended to help aid researchers in the areas of image processing and artificial intelligence.

The database consists of images of a total of one hundred and sixteen people, with sixty three of the images being of males and fifty three of the images being of females. Each subject has thirteen different images; each image contains a different pose or setting of the subject. The database contains images of Caucasian women, which includes women of a European and North American background [21].

Some examples of poses include:

- neutral expression
- smile
- anger
- scream
- left light on
- right light on
- wearing sunglasses
- wearing a scarf
- wearing scarf and left light on

The pose used in the research included only the neutral pose. The calibration in pose, illumination, and distance conditions of the images available from the database were ideal for the analysis. A total of 35 images of females were used from the database. The images used from the database were then resized to 800 pixels by 720 pixels and then converted to grayscale.

Figure 6: Sample Images from AR Face Database

3.1.2 Psychological Image Collection at Stirling

Several of the databases included in this research are part of a large collection of facial image databases at the University of Stirling in Scotland. Essentially meant as a public database for use in the study of the psychology of faces, the entire collection of databases is called the Psychological Image Collection at Stirling. There are a total of ten databases containing frontal images of various subjects in numerous poses and situations. In addition to these, the collection also includes two more databases which consist of images of children's drawings and man-made objects respectively [27].

The databases from this collection that have been utilized in this research include:

- Stirling Faces Database
- Nottingham Faces Database
- Utrecht ECVP Database

3.1.2.1 Stirling Faces Database

The Stirling face database consists of mainly monochrome images, with a total of 312 images of thirty-five subjects. Eighteen of the respondents were female and the rest were male, with each subject being photographed showing three different expressions and also

in three different poses. Moreover, the ethnicity of the female subjects is mostly British. This research made use of 10 images from this database, all of them in the neutral pose. The size of the images was modified to 800 pixels by 720 pixels and the images were consequently converted to grayscale during the normalization process [27].

Figure 7: Original images from Stirling database [27]

3.1.2.2 Nottingham Faces Database

Also part of the Stirling Collection, the Nottingham database contains 495 images of seventy-one subjects. Forty seven images of female respondents from this database were utilized for the purposes of this research. Each subject is photographed in four different poses, which include a frontal neutral view, two poses with a three-fourths view, and the last pose with a bathing cap over the hair.

The images are of female subjects of mainly the Great Britain region. The original images were monochrome and of the size 288 pixels by 384 pixels. This research operated on the images with the neutral front pose and the images were furthermore converted to

grayscale and resized to a standard resolution of 800 pixels by 720 pixels [27].

Figure 8: Original images from Nottingham database [27]

3.1.2.3 Utrecht Database

The Utrecht Database consists of images collected of subjects at the European Conference on Visual Perception held in Utrecht, Holland in 2008. There are a total of 131 images in the database, with forty nine of the subjects being men and twenty being women. Each subject has been photographed in two main poses, one neutral and one with the subject smiling.

The original resolution of the images was 900 pixels by 1200 pixels in color. However, the images were then reduced in resolution to 800 pixels by 720 pixels and converted to grayscale. Half of the subjects whose images were utilized for the research were from

Holland and the rest from other European ethnicities. Twenty images of women from the database were used in the research survey. The women were all in the neutral pose in the images [27].

Figure 9: Original images from Nottingham database [27]

3.1.2.4 FEI Face Database

The FEI face database consists of images collected at the Artificial Intelligence Laboratory at the Centro Universitário da FEI in Brazil. The database consists of 2800 images of 200 individuals. Each individual has 14 different images taken in various different poses, profiles and lighting conditions. The database contains images of 100 women and 100 men. The images were taken against a white homogeneous background and also included profile rotations of up to 180 degrees [41].

This research utilizes 74 images from the FEI Database, The original resolution of the images was 900 pixels by 1200 pixels in color. However, the images were then reduced in

resolution to 800 pixels by 720 pixels and converted to grayscale. The images that were used for this research had the subjects in the neutral pose.

3.1.2.5 Indian Face Database Beauty Queens

This database consists of face images taken of various subjects at the Indian Institute of Technology, Kanpur, India. The images are taken of 40 distinct subjects comprising of a total of 440 images in the database. These include 11 images taken for each of the 40 subjects as well as some additional photographs. The subjects are featured in various orientations, which include facing front, facing left, facing right, facing up, facing up towards left, and various others [42]. The subjects were also photographed displaying several expressions such as sadness, happiness and a neutral expression.

This research utilizes 11 images from this database. The images were converted to a resolution to 800 pixels by 720 pixels and subsequently converted to grayscale. The images that were used for this research had the subjects in the neutral pose.

3.1.2.6 Images of Beauty Pageant Contestants

The final set of images used for the purposes of this research consisted of images sourced from various publicly available databases containing images of beauty pageant contestants. These images were of pageants from earlier years of the pageant and were available for public use. The images used were taken from the Miss Universe and Miss World pageants dating back to 2003. A total of 18 images were included in this research to allow for representation of women that have been consciously selected for their beauty. This helps to establish a more verified set of images for the ground truth set.

3.2 Survey Methodology

In order to establish the ground truths for this research, it was very important to collect ratings from actual survey respondents. Thus, a survey was conducted and the results collected and analysed for the purposes of establishing accuracy and consistency standards for the research. The analysis also served the integral purpose of validating and supporting the hypotheses and assumptions made in this research.

The hypotheses include the following:

- consistency in attractiveness ratings between male and female genders
- cross cultural consistency and correlation in attractiveness ratings

3.2.1 Participants for the Survey

In this research, a survey was conducted, for the purposes of collection of attractiveness ratings, on several data sets of facial images of females. The volunteers consisted of a total of 48 people. Many of the participants were in the age group of 20 to 30 years. The volunteers were chosen so as to represent many diverse cultures and ethnic backgrounds and therefore the set consists of respondents from various countries.

Volunteers included 12 people of White Canadian background, which were made up of 4 men and 8 women. Furthermore, respondents included 4 females and 4 males of Chinese background, 4 females and 3 males of a Hispanic background, 4 females and 4 males of an Indian background, 3 females and 5 males of a British background, as well as 3 females and 2 males of a Japanese background. The data associated with the respondents, including the background, average age ranges, and etc. is shown in Table 2.

Respondent Background	Average Age	Number of Females	Number of Males
White Canadian	24	8	4
Chinese	24	4	4
Hispanic	25	4	3
Indian	23	4	4
British	25	3	5
Japanese	23	3	2

Table 2: Data related to the Survey Participants

The scope of the survey included participants of various backgrounds. A great number of the participants were international students at the university. This was of importance as they had exposure to both their own cultural conceptions of beauty and had, in addition, also been in contact with people from various backgrounds after having arrived in Canada. Thus, the respondents possessed experience and knowledge to make an informed decision with regard to the survey. Several of the students were also living in other countries abroad; this had the effect of making the respondent population diverse and accounted for variations in beauty preferences.

3.2.2 Data Set

Two hundred and fifteen gray scale photographs were used for the purposes of this survey. The photographs were presented in a grid format, with each photograph taking up one block of a 25 x 20 cm grid, with each block of size 4 x 3 cm. The data set consisted of images from several publicly available databases, with each database containing images of women from a different ethnic background. Thirty five images were used from

the AR face database, which contains mainly images of Caucasian women. A further forty-seven images were used from the Nottingham Face Database, which consists of images from women in Great Britain. Seventy four images were taken from the FEI Database, which contains images of women of Hispanic and Latin-American backgrounds. Twenty images were taken from the Indian Face Database, and ten images were selected from the Utrecht Face Database which contained images from several European countries. In addition to these images, a further twenty nine images were also added to the data set; these images were of women that had participated in beauty pageants from various countries around the world.

The variation in these images provides the desired group of images from an international sample of people. The mean age of the participants was centered around 24 years. The women in each image had a neutral face expression and did not wear glasses or any facial ornamentation. The images only revealed the face and the tops of the shoulders.

3.2.3 Procedure and Ratings Collection

Each respondent was provided with the entire collection of images, with the images randomly organized on an image grid. Individual respondents were provided with clear instructions regarding the survey methodology and purpose of research and were informed that their personal data would not be released. They were requested to examine and quickly scan all the images in the data set. Having done that, they were then asked to assess each image on the basis of facial attractiveness of each subject, being told specifically not to be biased by race or ethnicity. In addition, they were informed that their decision should be based on facial factors such as beauty and aesthetic factors.

The ratings were based on the Likert psychometric scale, which is designed explicitly for the validation and measurement of such personality traits and is often utilized for the purposes of psychometric surveys such as this. In this research, the use of a five-point Likert scale was decided upon, ranging from *attractive* being denoted by *5* on the scale to *unattractive* being denoted by *1*. Each respondent was asked to fill out the rating box below each image with the corresponding rating that was decided upon.

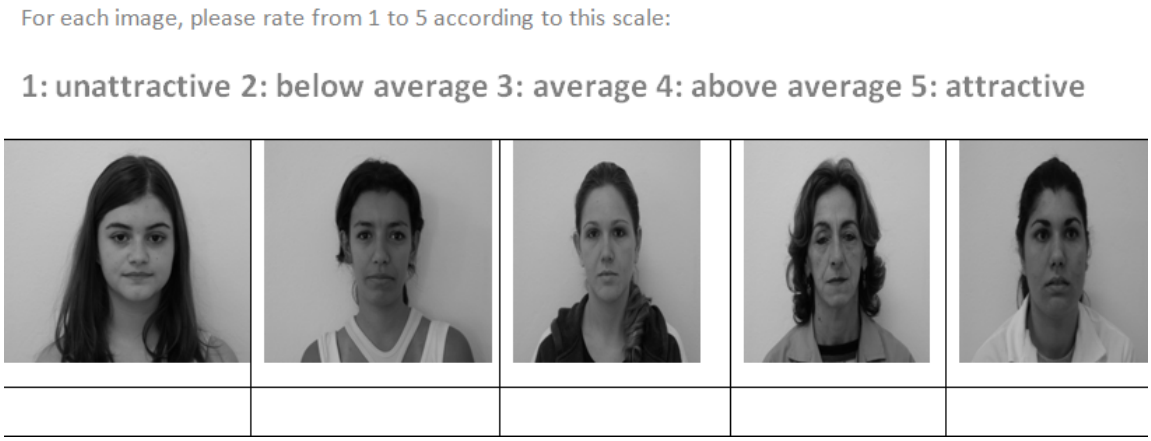

Figure 10: An excerpt from the survey

The scale used to rate the images is as follows:

1. unattractive
2. below average
3. average
4. above average
5. attractive

Several tendencies exist in respondents that this research tried to eliminate. These include a tendency of respondents to assign average marks in order to avoid offense to subjects. In order to eliminate this potential source of discrepancy, the respondents were informed

that their ratings were confidential and would not be released to the general public. Furthermore, many respondents were not sure what exact traits each rating corresponds to; this was eliminated by giving an explicit description associated with each rating.

Attractiveness Rating	Percentage of Images
5	17.2
4	22.6
3	22.2
2	20.9
1	17.2

Table 3: Percentage of Images at each Level of Attractiveness

3.2.4 Ratings Analysis

The analysis of attractiveness ratings is particularly essential as it allows for the validation and testing of several hypotheses and assumptions held in this research. Moreover, it provides significant correlations between attractiveness ratings and certain facial characteristics.

Two main assumptions regarding beauty and attractiveness were held during this research, the first one being that there exists a consistency in attractiveness ratings between the male and female genders. Secondly, it was also integral to the basis of this research that there exist a general agreement in between various cultures and ethnicities over beauty and attractiveness.

In order to test these assumptions, ratings were collection and analyzed for correlations and consistencies. These correlations are useful because they help in establishing patterns that can help establish a predictive relationship, which in turn can be used as the basis of

several experiments and research.

It was found that there was a strong correlation between the ratings of White Canadian males and females, with a correlation of r=0.89. There was also a strong correlation of ratings between most of the ethnic backgrounds except for the Indian respondents, for which the correlation was slightly lower than the rest of the population of respondents. Furthermore, cross-cultural correlations were analyzed for any significant results. This was done by analyzing the attractiveness ratings and calculating the mean ratings for the ratings given to an image by participants of a particular nationality or ethnic background. The findings are displayed below. The mean correlation between the groups was around 0.86, with a strong correlation in ratings between the white Canadian, British, Chinese and Indian respondents. There was a slightly lower correlation between the ratings of the Thai respondents and the rest of the respondent population.

Table 3 shows the percentage of images that were rated for each level of attractiveness ratings. The ratings are relatively normally distributed.

Chapter 4 Development of Representational Model for Assessing Facial Beauty

Despite remaining a topic of debate in our society, the area of facial beauty is one of constant research and development as beauty is one of the most central tenets of our society today. It has become essential to understand beauty and when possible, to improve it. However, in order to understand beauty, it is imperative to pinpoint the characteristics that are responsible for the expression of beauty present in human faces. Several characteristics contribute to the overall beauty and a methodology to evaluate and assess these features is presented in this thesis. Evaluating and assessing the extent of presence of these features is key to analyzing the beauty of a given face. These features include the location and geometry of various facial landmarks, skin composition and texture information, as well as overall image composition.

This section provides a description of the procedure followed for developing an overall representation of facial landmarks. The most effective procedure for analyzing and capturing the beauty content of a given image is through geometric features based on measured proportions, distances, and angles of the face. Thus, the geometric representation of the face is an essential component of the attractiveness analysis that is proposed. A key step in the geometric representation is the detection and extraction of facial features and landmarks. This step mainly comprises of normalizing the intensity distribution of the image, detection of facial regions and localization of facial feature points. These facial feature points include the points corresponding to the outline of major facial organs such as eyes, eyebrows, nose, and lips.

The recognition and beauty analysis algorithm can be significantly affected if the facial

points are located inaccurately. Therefore it is of the utmost importance to choose an algorithm that locates facial features and landmarks with a great level of accuracy. Other challenges that may be faced include images with resampling artifacts and external objects such as eyeglasses, hands, and jewelry.

Deformable models, a methodology used mainly for representing objects in the field of computer vision, were used to accurately represent faces in this research. Having been used in various fields for shape representation, this technique basically utilizes a set of known objects to analyze digital images. The main methodology is based upon approximation and geometry for the analysis.

In the context of this research, two main models were examined, these include Active Shape Models and Active Appearance Models. The Active Shape Model essentially tries to match a given set of points to an image using a statistical shape model, whereas the Active Appearance Model matches the position and texture of model points related to an image [45].

The algorithm for development of the facial representation is based on the Active Shape Model concept. Active Shape Models uses an iterative technique to match model points to a new image, which involves searching around each point to find a point nearby which best matches the model expected around that point. Then, the parameters which control point positions are adjusted in order to move the point closer to match the location of point in the image. The Active Appearance Model, on the other hand, generates a model of appearance which represents shape variation in the image, and then uses the differences between the current image model and target image to adjust its parameters [45].

The accuracy of both models was tested with various data sets. The results obtained with both models were compared with actual hand labeled points. For the data used in the scope of this research, the Active Shape Model located facial points with greater accuracy. In addition, the Active Shape Model also had a slightly lower runtime. The Active Appearance Model has a slightly larger capture range but the results become comparably better for the Active Shape Models as resolution is increased.

The methodology used in this research focuses on a specific deformable model technique known as Active Shape Models, developed by Cootes et al. The following chapter provides a brief overview of the procedure followed [45].

4.1 Active Shape Models

This section examines Active Shape Models and explains the main concepts and methodology followed in this research. Given an image of a face, the Active Shape Model essentially aids in the positioning of landmarks. Active Shape Models are essentially statistical models of given objects. When given an image of a new object, these models iteratively deform to fit to that object [45]. A training set containing labeled images is provided to the models and the shapes can only vary as much as and in ways that are seen in the training set. After the model is trained, the search for the features occurs.

4.2 Shapes

In the context of this research, a shape is essentially a set of landmarks on the face, which would be an array of x and y coordinates. Any Euclidean transformation such as an

expansion, rotation, or translation would still preserve the angles and any lines between the points and thus effectively retain the same shape. A 2-D shape S would be represented as a *2nx1* vector x containing the concatenation of each dimension as shown in Figure 11 below.

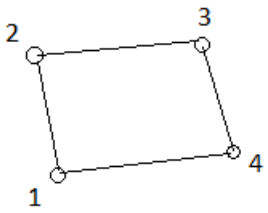

	x	y
Point1	2	1
Point2	1	5
Point3	6	6
Point4	8	2

$$\begin{matrix}2\\1\\6\\8\\1\\5\\6\\2\end{matrix}$$

Figure 11: A shape represented by a set of points connected by edges, a set of x and y coordinates and as a vector representation.

The distance between any two points on the shape is basically the Euclidean distance between the shapes calculated below [45].

$$d_E(\mathbf{x}, \mathbf{y}) = \sqrt{(x_1 - y_1)^2 + (x_2 - y_2)^2 + \ldots + (x_n - y_n)^2} = \sqrt{\sum_{i=1}^{n} (x_i - y_i)^2}$$

In order to solve for the Euclidean distance between Point 1 and point 2 in Figure 11, we can substitute the values for the coordinates in the equation as below:

$$d_E(\mathbf{x}, \mathbf{y}) = \sqrt{(2 - 1)^2 + (1 - 5)^2}$$

$$d_E(\mathbf{x}, \mathbf{y}) = \sqrt{17}$$

However, the distance between any two given shapes is the sum of the distances between

their corresponding points. The Procrustes distance between two shapes is the root mean square distance between the shape points.

4.3 Landmarks

The various features of interest in each image are called landmarks. Landmarks are usually chosen at clear corners of object boundaries, such as 'T' junctions between boundaries or biological landmarks.

Formally defined, “a landmark is a point of correspondence on each object that matches between and within populations”.

There are three main types of landmarks, which include anatomical landmarks, mathematical landmarks, and pseudo-landmarks. Anatomical landmarks have biological significance across organisms and are assigned by an expert. Mathematical landmarks are assigned to objects due to some mathematical property. The overall shape is represented by recording the connectivity between the landmarks to define how the landmarks join to form the boundaries of the shape.

Given landmarks labeled $\{(x_1, y_1), (x_1, y_2), \dots, (x_n, y_n)\}$. We can thus represent the n points as a single 2n element vector, x, where $x = (x_1, \dots, x_n, y_1, \dots, y_n)^T$. Given that we have P training examples, we will generate p such vectors x_j. Before any further analysis, the shapes must be all represented in the same coordinate frame [45].

4.4 Shape Alignment

To obtain a true representation of the shape, any effects due to location, scale, and rotational transformations need to be filtered out. In order to do this, a coordinate

reference is established and all the shapes are aligned to this reference [46].

The algorithm for the realignment of shapes is as given below.

Input: Unaligned training sets of shapes

1. Choose one shape as the initial reference shape
2. Translate each shape to be centred on the origin
3. Record the first shape to define the default orientation
4. Scale the reference shape to unit size, this is the initial mean shape
5. Align all shapes with the current mean shape estimate
6. Estimate the mean from aligned shapes again
7. Align the current estimate of the mean shape with the initial mean shape to constrain the orientation and scale to unit size
8. Convergence is achieved if the mean shape estimate does not show significant change. If convergence is not achieved, **return** to step 4.

The sum of the distances of each shape to the mean shape, which is given as shown below:

$$D = \sum |\mathbf{x}_i - \bar{\mathbf{x}}|^2$$

A reference shape is chosen and the remaining shapes are aligned accordingly. In order to minimize this distance D so that the shapes can be aligned, a similarity transform is applied. As this is a similarity transformation, only scaling, rotation and linear transformations are applied.

Thus, a similarity transformation that rotates the given point by θ, has a scale factor of s,

and an applied translation is as follows [46]:

$$T\begin{pmatrix} x \\ y \end{pmatrix} = \begin{pmatrix} x_{translate} \\ y_{translate} \end{pmatrix} + \begin{pmatrix} s\cos\theta & s\sin\theta \\ -s\sin\theta & s\cos\theta \end{pmatrix}\begin{pmatrix} x \\ y \end{pmatrix}$$

The shape is scaled by shrinking the size while preserving shape proportions. In addition, translation allows the shapes to have a common center, by moving each shape to its origin and subtracting the mass center of each point.

For the final step, we need to apply a rotation matrix, which in turn requires the calculation of a Singular Value Decomposition (SVD). The Singular Value Decomposition of a matrix is the decomposition of a given matrix = UDV^T, such that V is the eigenvector of A^TA and U is the eigenvector of AA^T [46]. For the rotation matrix of shape x_i in terms of x_j, the SVD of $x_i^T x_j$ is needed. The rotation matrix is then calculated as follows:

$$VU^T = \begin{bmatrix} \cos\theta & -\sin\theta \\ \sin\theta & \cos\theta \end{bmatrix}$$

The Active Shape Model (ASM) is trained on a set of manually landmarked images before training begins. After the training, the ASM is used to search for features on a face. The general approach is to try to locate the landmarks independently and then correct the locations by observing the relationship between the landmarks' locations [46]. The ASM is constructed from two main sub-models: the profile model and the shape model. The shape model acts globally, while the profile model acts locally.

4.5 Profile Model

The profile model specifies what the overall image is supposed to look like around a

particular landmark on a given face. Its main task is to formulate a shape for a given face approximation by template matching at the landmarks.

The profile model is based on profile vectors, which are one-dimensional vectors which describe the characteristics of the image around a given landmark. The area around each landmark is sampled in order to build a profile model for the particular landmark, after sampling the vector is then again moved to the position that best corresponds to the landmark's model profile.

The profile vector **g** at a given landmark is formed by sampling intensities along a one-dimensional vector which is orthogonal to the shape edge. This vector is often referred to as a whisker, as it is a small vector containing a small set of intensities found in the neighborhood of a shape edge. This is illustrated in Figure 12 below [47].

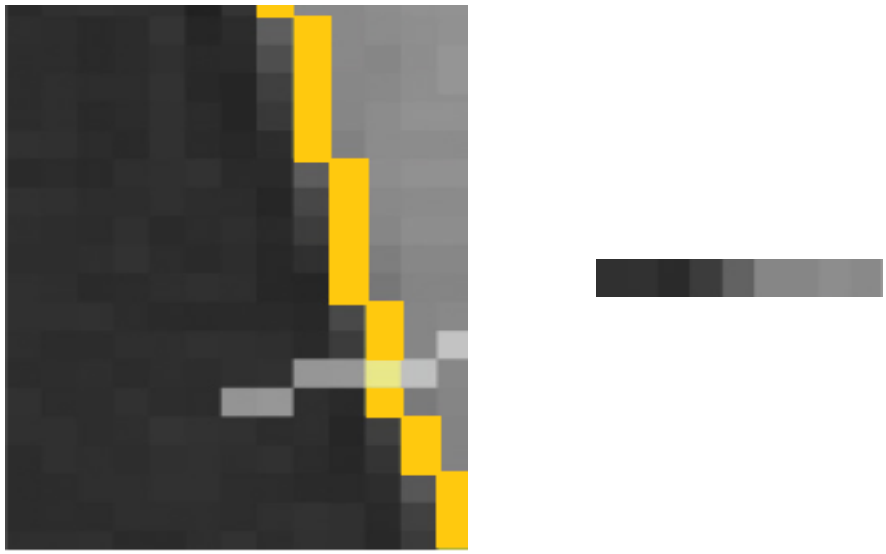

Figure 12: Example of construction of profile vector

The yellow line represents the edge of a particular shape. The gray line orthogonal to the edge is the whisker; the landmark is located at the intersection of the two lines. The profile vector is derived from the whisker vector at the boundary and after going through

a set of normalization steps, contains the values desired.

The profile vector, g, is formed through a set of steps. Initially, the elements of the profile vector are set to the intensity values of the image below it. Then, each profile element is replaced with the value found by calculating the difference between its own value and the value of the previous element. Each element is then divided by the sum of the absolute values of all vector elements. These normalized gradients have the effect of lessening varying image lighting and contrast [47].

4.6 Shape Model

The ASM shape model essentially defines the allowable positions of landmarks. This model helps to adjust the shape suggested by the profile model to match a legitimate face shape, making this an integral component because profile matches at landmarks are often unreliable. Before building the model, it is important that the shapes be aligned.

The shape model is made up of two components: the average face and the allowable distortions on the average face [46]. This is represented by the following equation:

$$\hat{x} = \bar{x} + \phi\, b$$

The mean shape $\bar{x}$ is defined as follows [46]:

$$\bar{x} = \frac{1}{n_{\text{shapes}}} \sum_{i-1}^{n_{\text{shapes}}} x_i \,.$$

Here $\hat{x}$ is the shape vector generated by the model, $\bar{x}$ is the average of the aligned training shapes x_i, and Φ represents the matrix of eigenvectors of the covariance matrix S of the training shape points [47].

The covariance matrix is calculated as follows:

$$\boldsymbol{S}_s = \frac{1}{n_{\text{shapes}} - 1} \sum_{i-1}^{n_{\text{shapes}}} (\boldsymbol{x}_i - \bar{\boldsymbol{x}})(\boldsymbol{x}_i - \bar{\boldsymbol{x}})^T$$

Thus the equation [top of page] can be used to model different shapes by varying the main vector parameter b. By ensuring that the values of $\boldsymbol{b}$ fall within known limits, the model generates lifelike faces. The limits fall between $-3\sqrt{\lambda_i}$ and $3\sqrt{\lambda_i}$, where λ_i is the *ith* eigenvalue of S. Figure 13 below shows the generated mean face shape model represented with the solid black line and the several variations on the shape model represented with gray lines [45].

Figure 13: The mean face shape model (black line) and the variations on the model (gray lines)

4.7 ASM Image Search

After the completion of the models, they can be used to located regions of faces in new input images. Cootes et al [47] defined an algorithm to find the adapted shape *x,* given a target shape y, by fitting the constructed model $\hat{x}$ to the new set of points [47]. During this search, several searches are constructed by sampling the image in the neighborhood

of each landmark. The algorithm for ASM Search is as follows:

Input : Face Image

1. Generate the start shape by locating the overall position of the face
2. Sample the area around the offset to build a profile and measure the fit of the profile against the profile model built
3. Move the point to the offset of the best profile match
4. Adjust the suggested shape to conform to the Shape Model
5. Repeat until convergence, which means until no further improvements are possible

Output: Shape with (x,y) coordinates of face landmarks [46].

4.8 Fitting Generated Model to Given Points

The key parameter used to build a given model is b, which is the shape parameter. One specific value of b corresponds to one specific form of the model, which can be turned into the corresponding shape by using the transformation from the model's coordinate frame to the image's frame. In order to fit a particular model to new points, we must first initialize all the shape parameters to zero.

Any instance of the model is represented by

$$\hat{x} = \bar{x} + \phi b.$$

The model instance is then generated and the set of parameters that minimizes Δx is computed and is given by $y\text{-}T(x)^2$. Here T is the similarity transformation described below:

$$T\begin{pmatrix} x \\ y \end{pmatrix} = \begin{pmatrix} x_{translate} \\ y_{translate} \end{pmatrix} + \begin{pmatrix} s\ cos\ \theta & s\ sin\ \theta \\ -s\ sin\ \theta & s\ cos\ \theta \end{pmatrix} \begin{pmatrix} x \\ y \end{pmatrix}$$

Thus the positions of model points in an image X are given by:

$$X = T_{(X,Y,S,\theta)}\ (\bar{x} + Pb)$$

The best fitting model instance minimizes the sum of square distances between the corresponding model image and points and is equivalent to the following expression [47]:

$$Y - T_{(X,Y,S,\theta)}\ (\bar{x} + Pb)^2$$

Figure 14 below shows the final model fitted to one of the images part of the database.

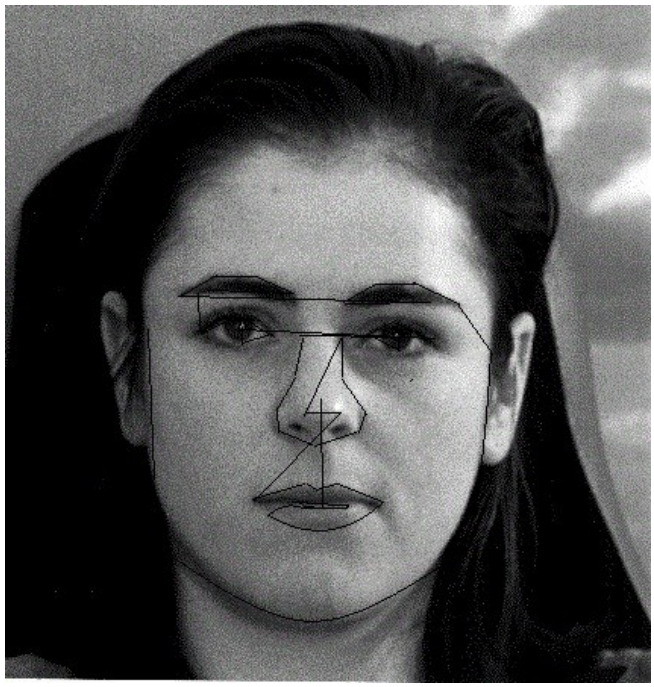

Figure 14: Final fit of model to a sample image

4.9 Processing Results

The Active Shape Model is utilized for the extraction of facial features. This method is

quite efficient in locating various landmarks on the face and being able to extract the position of the corresponding landmark. However, the input needs to be an image with a good resolution quality as the output of the algorithm is greatly improved when image quality improves. The processing contains errors when the image is not of a consistent variation such as when the person is wearing glasses.

Furthermore, the training of the model is highly dependent on the initial landmarks input into the algorithm. Therefore, the accuracy is often constrained by the initial precision of landmark placement. After running the algorithm for several variations of inputs, the best results were obtained with images of a resolution of 800 by 720 pixels. The convergence of the algorithm occurred after 17 iterations for the final run of inputs. With an overall likelihood of error occurring for around 2 percent of images, the algorithm provided generally consistent results.

Chapter 5 Formulation of Algorithm for Beauty Analysis

Feature selection is one of the most important steps that affect the accuracy of analysis. The selection of features is dependent upon what characteristics play a role in the formulation of a representation that exemplifies the integral components of human beauty. This determines the validity and accuracy of results. In the scope of this research, the features used have been chosen to develop an effective representation of the essential components of the human face. The main challenge has been in selecting what aspects of the human face inherently contribute to the perception of beauty. The challenge has been in the quantification of the identification of beauty.

Various theories of beauty exist in order to aid the understanding of this concept. The geometric representation of a face often helps to identify the key components of a given face. In addition to this the texture of a face is of importance in relation to beauty. Furthermore, the overall shape of the face must be represented as well in order to complete the description.

This chapter outlines the overall implementation and methodology proposed by this research. The proposed algorithm represents the face using various key characteristics. The features extracted help to represent facial characteristics in three major areas. Geometric features help to represent the symmetrical properties and ratio-based properties of landmarks on the face. Textural features extracted help capture information related to skin texture and composition. Finally, face shape and outline features help to categorize the overall shape of a given face, which helps to represent the given female face shape and outline for the further analysis of any deviations from the basic face shapes. The algorithm is made up of sub-modules for each of these sets of features. Each

module has been developed as part of this research and is a novel contribution. The system is outlined in Figure 28, which shows the significant components and steps followed to establish the system.

5.1 Facial Representation

Beauty analysis is highly dependent upon the representation of the face that is provided to the classifier. The more realistic the representation, the more accurate the results will be. Hence, the chosen features must be accurate and integral components of the real world representation of beauty and of the processed data as well.

In the approach of this research, the Active Shape Model is proposed for the extraction of facial landmarks, which has resulted in an accurate set of landmarks and their positions. The Active Shape Model algorithm is used as the foundation of the overall algorithm developed for extracting the major landmark positions. The Active Shape Model concept was adapted for accurate analysis of facial features, thus the algorithm was developed using the model. The model obtained was then trained specifically for the databases utilized in this research.

After extracting the positions of landmarks, the feature vector must be prepared for training purposes. The contents of the feature vector depend on the combination of beauty analysis algorithms. This research proposes an accurate representation of natural facial beauty. This involves the geometric representation of facial landmarks, texture analysis, as well as edge histogram information.

In order to extract features from a given image, it is often important to locate key landmarks on the image in order to further process those landmarks for the formation of

features.

The model was initially trained on the Nottingham Face Database, as it was an accurate representation of the resolution and size of the other datasets in the research.

For detecting parameters using this model, it is important to align them in order to obtain good results. The process has been outlined in detail in Chapter 4. However, the following explanation presents a brief summary. The main steps taken for the alignment are as follows:

1. Selection of reference shape, letting $\mu_1 = x_1$
2. Translation of each shape to centre it on origin, $\mu_i = T(x_i)$, which is essentially for pose correction.
3. Scale reference shape to unit size
4. Recalculate mean shape from aligned shapes
5. Constrain mean shape and align μ_0
6. Iterate until convergence

After the alignment of the training set has occurred, the shape must be modeled. The mean shape $\bar{x}$ and the covariance matrix $\sum x$ are computed from the aligned training set by the application of Eq 5.1:

$$\bar{x} = \sum_{i=1}^{N} x_i \tag{5.1}$$

The covariance matrix is computed as follows:

$$\sum x = \frac{1}{N}\sum_{i=1}^{N}(x_i - \bar{x})(x_i - \bar{x}) \tag{5.2}$$

As demonstrated earlier, the shape model is represented as $x = \bar{x} + \phi\, b$. Here x is the shape vector generated, ϕ is the set of eigenvectors of the covariance $\sum x$ and b

represents the parameter for the shape vector.

The final step involves fitting the model that has been constructed to a new set of points, which can be represented by z. Each shape has its own characteristic parameter b, which is set to zero when first fitting a set of points. Thus, the following steps are further followed:

1. Model instance is represented by $x = \bar{x} + \phi\, b$
2. Find parameters which best align model points, parameters include: $X_t,\ Y_t,\ s, \Theta$
3. Invert the transformation of T(y) to get $y' = T^{-1}(y)$
4. Update the parameter of b and apply constraints.
5. Iterate until convergence [46]

These steps are necessary for fitting the new set of points to an already existing model. Figure 13 shows the results of the various iterations performed until a fit is achieved. For each image, the landmarks were initially detected directly on the image itself, and then the map of labeled points was scaled to a coordinate system. Finally, a computer application was programmed to compute each of the measurements associated with the geometric feature vector.

5.2 Geometric Features

Geometric features play a key role in the analysis of the beauty content of a face. In order to extract the geometric features, each face had to be landmarked. The landmarking process required images to be of a certain quality in order for the results to be of the highest accuracy. Various image sizes were experimented with in order to find the size that resulted in most accurate feature extraction. The size that was found to result in the

best extraction results was 800 pixels by 720 pixels. Table 4 below shows the various sizes tested and their respective results.

Size	**Accuracy Results (%)**
450 pixels by 350 pixels	68.3
640 pixels by 560 pixels	77.1
800 pixels by 720 pixels	85.0

Table 4: Sizes tested with their corresponding results

Various geometric features were extracted from each face in order to form an accurate representation. The extraction of features was implemented in C. The focus was on choosing features that would result in the highest accuracy when testing with the sample data set. After undergoing several tests, a feature vector containing the select features which effectively described the feature set was constructed. The following sections will describe in further detail the various components of the features vector.

A total of 62 landmark points were selected for each facial image. The landmark points contained various sub categories corresponding to regions of the face. For example, a total number of 15 points represented the outer outline of the face, 6 points represented each eyebrow, etc; these are illustrated in the diagram outlined in Figure 15.

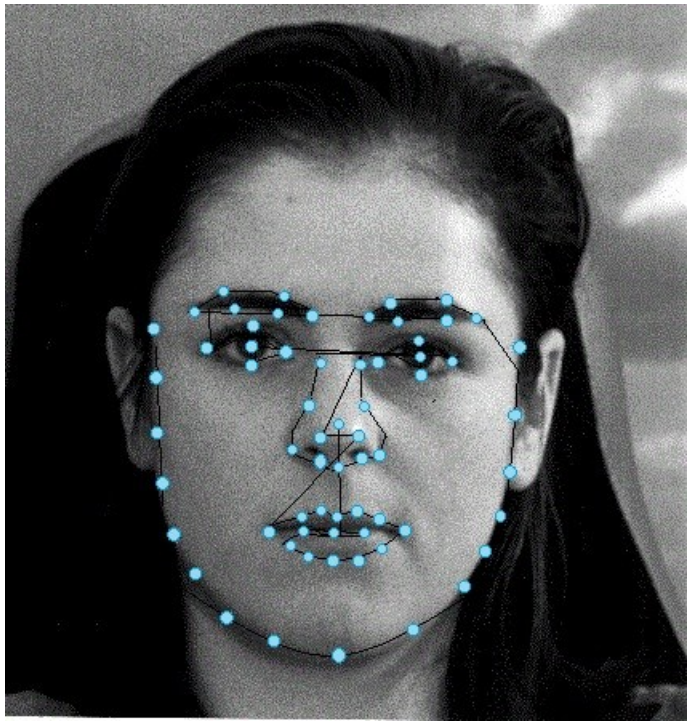

Figure 15: Facial landmarks outlined

The various sub modules containing landmarks of the face are as follows:

Outline of Face:	15 landmarks
Left Eye:	5 landmarks
Left Eyebrow:	6 landmarks
Right Eye:	5 landmarks
Right Eyebrow:	6 landmarks
Nose:	10 landmarks
Nostrils:	2 landmarks
Lips:	12 landmarks

For each image, the landmarks were initially detected directly on the image itself, then the map of labeled points was scaled to a coordinate system. Finally, an automatic

computer application was generated to compute each of the measurements associated with the geometric feature vector. The final results of this application were then analyzed for the purposes of inclusion in the final feature vector.

5.2.1 Ratios Pertaining to Major Facial Regions

The combination of features from various theories of facial beauty makes the proposed algorithm unique. The algorithm for the geometric features sub-module has two main parts. The first section contains basic measurements taken of various regions of the face, while the second section extracts features based on various theories of beauty.

This section elaborates on the basic measurements taken of various regions of the face. Section 5.2.2 will elaborate further on the features associated with various theories of beauty.

The first set of ratios to be discussed mainly involves ratios extracted from the major facial regions. These regions include the eye region, the nose region, and the mouth region. Each region was analysed and a number of associated measurements and ratios were extracted for each respective region. The following sections help to outline these measurements.

5.2.1.1 Eye Features

Before coming up with the final set of feature vector for the eyes, several combinations of features were experimented with. Initially, the overall size of the eye was represented in terms of the landmark points that formed the outline of the eye. This effectively meant that rather than calculating the width or height at only a certain point of the eye, all the

points that were part of the outline of the eye were taken into consideration. Using this set of points as part of the final training vector, the classification results demonstrated an accurate classification percentage of around 67%.

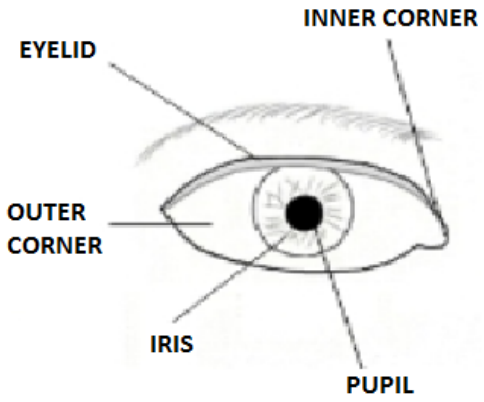

Figure 16: Detailed diagram of eye [56]

It was evident that this number could definitely be improved upon. The features that were used next for the vector consisted of specific distances that were measured for various parts of the eye. Some of the specific measurements that were extracted are shown below in the table; these are mainly relationships between the iris, pupil, and corners of the eye. In addition to this, the relationships between the eye and its surrounding facial features were also considered; these included relationships between the eye and the eyebrow, the eye and mouth corners, the eye and the nose tip, the eye and the face outline [56].

The table below, Table 5 outlines the various features that were used from the eye. In order to make the descriptions more clearly, Figure 16 illustrates the various terminologies and parts of the eye mentioned in Table 5.

Feature Extracted From Eye	Inclusion in Final Feature Vector
Horizontal distance between inner corners of eye	Yes
Horizontal distance between outer corners of eye	Yes
Horizontal distance between pupil and iris	No
Horizontal distance between pupil and outer corner of eye	No
Horizontal distance between pupil and inner corner of eye	No
Vertical distance between eyelid and eyebrow of eye	Yes
Horizontal distance between iris and left corner of eye	Yes
Horizontal distance between iris and right corner of eye	Yes
Vertical distance between outer corner of right eye and mouth corner	Yes
Vertical distance between outer corner of left eye and mouth corner	Yes
Horizontal width of iris	Yes
Horizontal distance between eyes	Yes
Vertical distance between pupil center and eyebrow	Yes

Table 5: Features related to the eye

5.2.1.2 Nose Features

Another key component of the face is the nose. Therefore, an accurate representation of the nose has the potential to significantly contribute to an accurate representation of the face. Several characteristics were initially extracted from the positioning of the nose. The measurements included the lengths of the diagonals that can be constructed and the vertical and horizontal lengths [57].

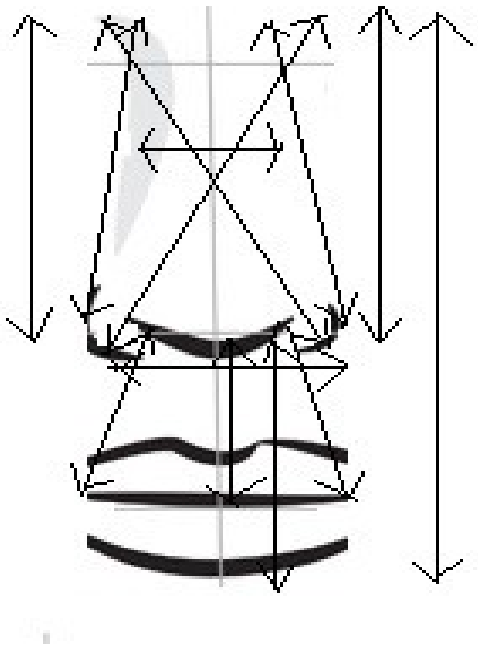

Figure 17: Various measurements taken of the nose [57]

The width of the nose at the midpoint of the nose was also considered; the measurements are outlined in the table below. Of importance is the computation of the nose area, which is a significant characteristic of the nose and helps to greatly improve the training results.

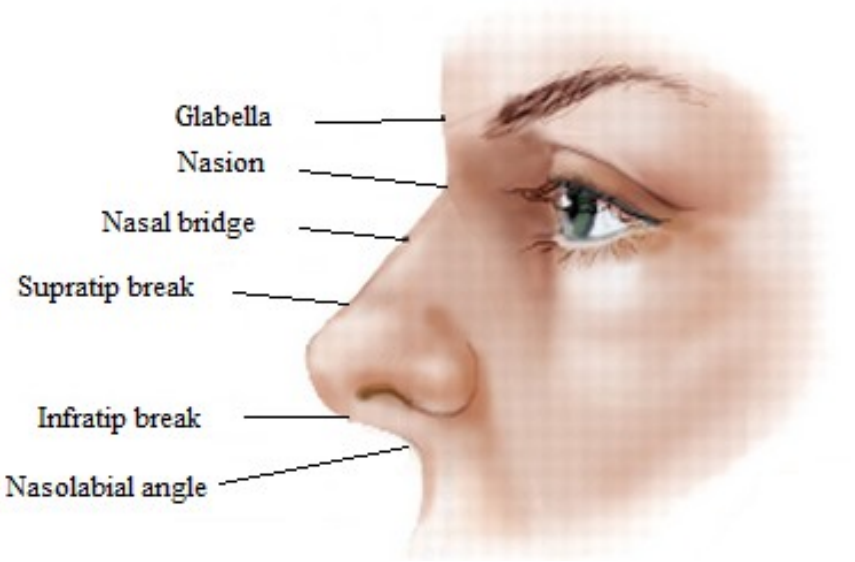

Figure 18: Major features of the nose

In addition, various ratios taking into account measurements for the nose in relation to measurement taken of other face features were computed. These ratios basically viewed the nose in relation to the other facial features, and they are outlined in Table 6 below. In addition, Figure 18 shows the anatomy of the nose and the various parts of the nose that were used as part of the measurements are labeled. These descriptions are used to help elaborate on the exact measurements that were taken to form the final features used in the feature vector.

Feature	Inclusion in Final Feature Vector
Horizontal distance between two nostrils	Yes
Horizontal width of protrusion of nose	Yes
Vertical length of nose from glabella to infratip	Yes
Nose area	Yes
Vertical length between glabella to bottom edge of lower lip	No
Diagonal length from the nasion to right nostril of nose	No
Diagonal length from the nasion to left nostril of nose	No
Diagonal length from the left nostril to left corner of mouth	Yes
Diagonal from the right nostril to right corner of mouth	Yes

Table 6: Ratios related to the nose

5.2.1.3 Mouth Area Features

The last component of the face that was analyzed was the mouth area. This area consists mostly of the lips; the relationship between the lips and the rest of the face is also observed. The landmarks forming the outline of the lips were located and they form part of the feature vector. In addition to these, several other features associated with the lips were extracted. These include the thickness of the upper and lower lip, the horizontal length of the lip, various ratios pertaining to the lip in relation to other facial features. The ratios and other major features are presented in Table 7 below.

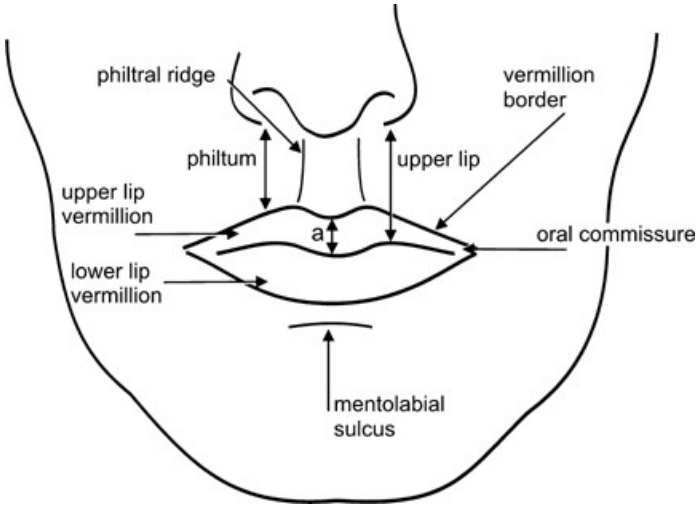

Figure 19: Landmarks of the mouth

When analyzing the features related to the lips, it was important to eliminate some features that did not contribute effectively to the feature vector and in some cases decreased the accuracy of the representation [58]. Features that were eliminated included the midpoints of the lips and line representing the division between the upper and lower lip. The landmarks of the mouth that were part of the feature vector are illustrated in Figure 19. Consequently, these landmark names are used to further describe the ratios in Table 7 which were obtained for the final feature vector.

Feature	Inclusion in Final Vector
Vertical distance between oral commisure to center of face	Yes
Vertical thickness of upper lip= difference between length from nose until oral commisure and length from nose until upper lip vermillon border	Yes
Vertical thickness of lower lip= difference between length from nose until oral commisure and length from nose until lower lip vermillon border	Yes
Vertical distance between upper lip vermillon border and chin	No
Vertical distance between lower lip vermillon border and chin	Yes
Vertical distance between nose tip and upper lip vermillon border = Philtum	No
Lip area of upper lip = total skin area of upper lip	No
Lip area of lower lip = total skin area of lower lip	No

Table 7: Ratios related to the mouth

5.2.2 Ratios Pertaining to Facial Beauty Theories

The representation of facial beauty is based on several maxims of beauty that have been established over the years. The Golden Ratio and Facial Thirds methods have been used when formulating a geometric representation. In addition to these methods, five more ratios have been added that have improved the representation of the face greatly. This has even led to various plastic surgeons and scientists applying these methods to their practices.

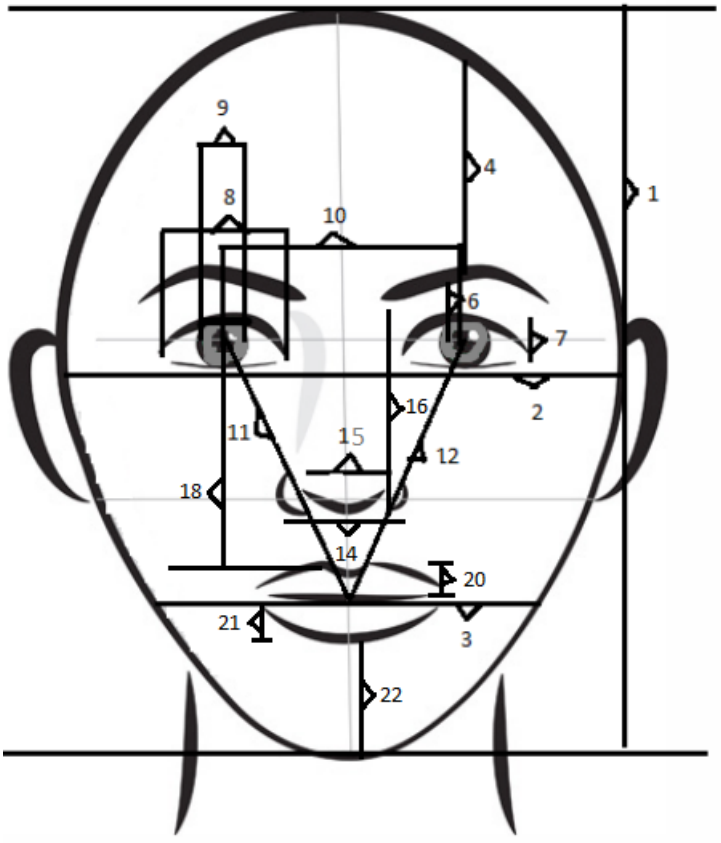

Figure 20: Representation of measurements from Table 8

The Golden Ratio is approximately the ratio of 1.618 to 1. According to the Golden Ratio, all the proportions described in Table 9 must fit this value in the case of a perfectly aligned ideal face. The various geometric features that were extracted from each face are shown in the Table 8 below. Many of these features are further used for the calculation of these proportions in Table 9.

Measurement ID	Description
1	Vertical distance between top of forehead and chin
2	Horizontal distance between outer edges of cheekbones
3	Horizontal distance between outer cheeks at the mouth
4	Vertical distance between eyebrow and hair
5	Vertical height of upper head including hair (not shown)
6	Vertical distance between pupil center and eyebrow
7	Vertical distance between upper and lower edge of eye
8	Horizontal distance between inner corner and outer corner of the eye
9	Horizontal width of iris
10	Horizontal distance between centre of pupils
11	Diagonal distance between left eye and center of the mouth
12	Diagonal distance between right eye and center of the mouth
13	Average cheekbone prominence calculated by evaluating the difference between width of face at cheekbones and width of face at the mouth (not in image)
14	Horizontal distance between the two nostrils
15	Horizontal width between two protrusions of the nose
16	Vertical length of nose
17	Nose area: product of length of nose and the width of the nose at the tip (not in image)
18	Length of the midface: Vertical distance between center of pupil to upper edge of lip
19	Horizontal width of cheeks (not in image)
20	Vertical thickness of upper lip
21	Vertical thickness of lower lip
22	Vertical distance between lower lip and chin

Table 8: Measurements taken for Geometric Representation of Face

The measurements are illustrated in Figure 20. As can be seen in the figure, various

measurements are taken which include characteristics from both the Golden Ratio methodology and the Facial Thirds methodology.

These features represent a portion of the final feature vector that will be trained against the training sets. However, there are several more features that are calculated according to established ratios for facial beauty. These features are based on the Golden Ratio and Facial Thirds methods described earlier.

The measurements taken based on the Golden Ratio theory are explained in the table below.

Ratio ID	**Description**
1	Vertical distance between pupils and tip of chin: vertical distance between top of face and pupils
2	Vertical distance between face and nose: vertical distance between nostrils and tip of the chin
3	Vertical distance between pupils and central lip line to vertical distance between lips and top of the chin
4	Vertical distance between nostrils and tip of the chin to vertical distance between pupils and nostrils
5	Vertical distance between pupils and nostrils to vertical distance between nostrils and lip line
6	Vertical distance between lips and top of the chin to vertical distance between nostrils and lip line
7	Mean of the above ratios

Table 9: List of Ratios Associated with the Golden Ratio

5.2.2.1 Features based on Facial Thirds Method

In addition to the above measurements, the Facial Thirds method was further utilized to extract several meaningful features which helped to further develop an accurate representation of the face. The Facial Thirds method states that any well proportioned face can be divided into equal thirds by drawing lines that separate the various regions on the face. These lines are drawn through the hairline, the eyebrows, the base of the nose and the edge of the chin. In addition to these requirements, it is also essential that the distance between the lips and the chin be double that of the distance between the base of the nose and the lips.

The facial thirds divides the face in proportional regions, as can be seen in Figure 21.

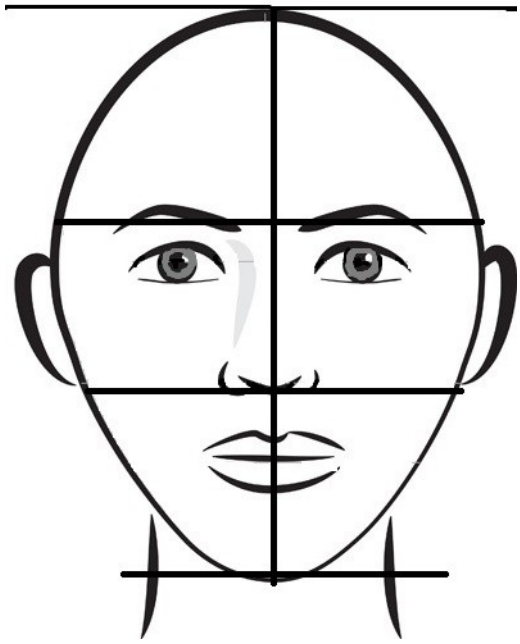

Figure 21: Facial Thirds: The three regions on a face

The table below summarizes the various ratios are proportions that should be satisfied by a face that is in accordance with the Facial Thirds theory.

Ratio ID	**Facial Thirds Ratio Description**
1	Vertical distance between top of face and eyebrows : face length
2	Vertical distance between eyebrows and tip of nose
3	Vertical distance between tip of nose and centre of the line joining the upper lip
4	Vertical distance between top of nose (area between the eyebrows) and lips to vertical distance between lips and the tip of the chin

Table 10: List of Ratios Associated with the Facial Thirds theory

These ratios complete the geometric features component of the feature vector. Further,

the texture component and the edge histogram component will be seen in greater detail.

5.3 Texture Analysis

The algorithm developed for analysis of facial texture makes use of statistical textural models to extract key textural features of the face. Statistical textural models have not yet been used for the analysis for facial beauty in image processing. This novel proposed algorithm for textural analysis is key for developing an accurate facial model of beauty as the accuracy of the overall algorithm is increased by 20% percent with the use of this sub-module.

Texture is an integral component of any given image as it represents the surface and structural qualities of the image. Texture is often defined as a regular repetition of an element on a given surface. Image texture mostly consists of complex patterns that give the image its unique characteristics of brightness, color, shape, size, and many more.

Texture is often one of the main features utilized to describe the structure of a given object. Images are basically made up of pixels and texture is essentially the relationship between these pixels. Texture is often quantified through descriptors such as smoothness, coarseness, and regularity; these help to provide a measure of the textural properties of an object.

The texture element in a human face refers to the level of smoothness that is perceived. There is considerable correlation observed between the smoothness of a skin and the overall attractiveness associated. Face with smooth skin texture that is free from blemishes, spots, flakiness, rough patches, acne and any unwanted scars is considered desirable and generally ideal. Therefore, it is imperative that the feature vector associated

with a given image also take into consideration the texture elements present.

Figure 22: Various textures represented

Texture is a quantitative measurement of the arrangement of intensities in a region and it can be characterized through various methods. The methods fall into three main categories: statistical, spectral, and structural methods [52].

Statistical methods mainly describe an attribute texture through the statistical distribution of the intensities of the image; this is done through the analysis of distribution of gray value intensities in a given image.

On the other hand, spectral methods base themselves on the properties of the Fourier spectrum and essentially identify high-energy and narrow peaks. These peaks are then used to detect the various periods present in the overall image. Furthermore, structural techniques are associated with the arrangement of basic image components and thus describe texture based on the spacing between lines in the image. These methods are apt for images with textures that have many varying properties.

The initial approach to texture analysis included both spectral and statistic approaches. The spectral approach was considered as it would help to represent any major patterns occurring in the image, basically helping to establish any global patterns that were present. The basis of the spectral approach is on three key observations. The Fourier spectrum is ideally suited to represent global texture patterns in an image. The three main aspects of the spectrum that are important for texture analysis are:

- Large peaks in the Fourier spectrum describe the principal direction of texture patterns.
- Location of peaks gives the spatial pattern of textural patterns.
- After periodic elements are eliminated, the result is an image that can be further described by statistical techniques.

The detection of textural components of an image is done by expressing the Fourier spectrum in terms of polar coordinates. This results in two functions, *S(r)* and $S(\theta)$, where S is the Fourier spectrum function and r and θ are the variables of the coordinate system.

The entire global description is obtained through the following equations [52]:

$$S(r)=\sum_{\theta=1}^{\pi} S_{\theta}(r) \tag{7.3}$$

$$S(\theta)=\sum_{r=1}^{R_0} S_r(\theta) \tag{7.4}$$

Thus, these functions essentially describe the textural aspects of the various regions of the image under consideration. In order to further quantitatively characterize the behavior of these functions, various descriptors are calculated. These include the highest value, the

mean and variance of the axial functions, and the distance between the mean and highest value of the function. These are essentially the features that were considered for the feature vector. However, after testing with these features, it was found that only a few actually contributed effectively to the overall representation. Thus, these were retained and the rest of the features were eliminated from the feature vector. The features that were kept were those with the highest value of each function.

The main textural features utilized in this research are statistical textural features. This specifically refers to the use of statistical moments of the image's intensity histogram to describe texture.

A statistical moment is essentially a quantitative measure of a set of points. Assuming *z* to be a random variable which represents the intensity and i = 0, 1, 2.... L-1. Here $p(z_i)$ is the corresponding histogram for these intensity levels and L is the number of distinct intensity levels. The average intensity value, m, of z is computed by:

$$m = \sum_{i=0}^{L-1} z_i \, p(z_i)$$

In addition, the nth moment of z with respect to the mean is calculated as follows:

$$\mu_n(z) = \sum_{i=0}^{L-1} (z_i - m)^n \, p(z_i)$$

The second moment is of great importance in texture description as it is a measure of intensity contrast that in turn is used to describe the amount of relative smoothness present in a particular image. The second moment is essentially the variance, which is also represented as:

$$\sigma^2(z) = \mu_2(z)$$

Here it is important to note that $\mu_0 = 1$ and $\mu_1 = 0$. The variance is normalized to a value between 0 and 1 as the values tend to be in a very large interval [53].

The variance is used to describe the texture through descriptors such as the value of R, which is given below:

$$R = 1 - \frac{1}{1 + \sigma^2(z)}$$

The value of R is 0 for areas of constant intensity. The value of R approaches 1 for areas of rough textures. The third moment is essentially a measure of the skewness of the histogram and a good indicator of texture properties. It is calculated with n=3, as below:

$$\mu_3(z) = \sum_{i=0}^{L-1} (z_i - m)^3 p(z_i)$$

It is important to observe the uniformity of the histogram as that is often shown to be an indicator of texture. The measure of uniformity is further then calculated using the following:

$$U = \sum_{i=0}^{L-1} p^2(z_i)$$

The value of U is maximum in an image in which all intensity values are equal, meaning it is maximally uniform. A further measurement is taken in terms of the entropy content of an image. Entropy is a measurement of the amount of variation present in an image. The value for an image that has constant intensities is 0. The measure of average entropy is as follows:

$$e = -\sum_{i=0}^{L-1} p(z_i)\log_2 p(z_i)$$

We can illustrate this procedure with the use of an example. Let's use the intensity histogram below for this example.

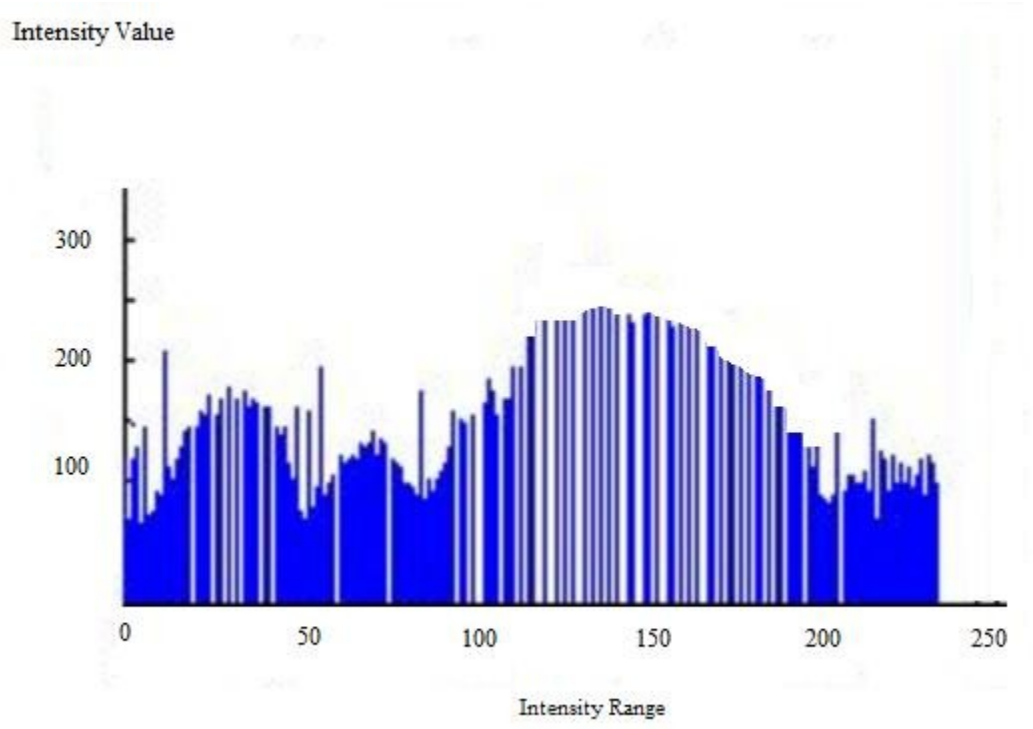

The value for the mean for this particular image is calculated by the average of all the intensity values as illustrated by the equation below:

$$m = \sum_{i=0}^{L-1} z_i p(z_i)$$

This provides us with a value of 147.12. Furthermore, we must calculate the variance as variance is an accurate measure of texture. Given a 5 X 5 region of the image for a specific calculation, the variance is:

$$T_v(x,y) = \frac{1}{25}\sum_{s=-2}^{2}\sum_{t=-2}^{2} |g(x+s,y+t) - \bar{g}|^2$$

Here g represents the positional differences in the x and y direction. Thus, s represents the positional difference in the x direction and y represents the positional difference in the y direction.

$$\bar{g} = \frac{1}{25}\sum_{s=-2}^{2}\sum_{t=-2}^{2} g(x+s,y+t)$$

This provides us with a value of 0.088139 for the variance. The variance tends to be large for grayscale images; therefore, this was normalized using the value of g. This helped to keep the result in the range [0, 1].

In addition, we must calculate the value for texture descriptor R, which is calculated as below: 0.081

$$R = 1 - \frac{1}{1+\sigma^2(z)}$$

Substituting for the value of variance, we get:

$$R = 1 - \frac{1}{1+\ 0.0881}$$

This provides us with a value of 0.081 for the texture descriptor R.

The above measures help to represent the overall texture of an image. In this research, the texture of an image is seen as a significant indicator of the attractiveness ratings that it should be associated with. After conducting the study, the results were analyzed and the texture analysis performed on the various datasets were assembled for the study. The

intent was to observe any correlations between texture analysis values and the attractiveness ratings collected [53].

The analysis showed that there was indeed a correlation between the texture components and the perceived beauty content of an image. The major components of the results are shown in Table 11.

Description/Rating	**Mean**	**Third Moment**	**R(normalized)**	**Entropy**
1: unattractive	193.61	89.43	0.09	8.78
2: below average	179.7	68	0.08	7.71
3: average	112	47	0.05	6.68
4: above average	97	31	0.02	5.3
5: attractive	89	28	0.01	5.1

Table 11: Textural features obtained

The values obtained Table 11 outline some of the results obtained for each of the statistical moments and characteristics described earlier. These were calculated for the images that were part of the dataset for the research. The values described earlier were all found for the data sets, however, not all were found to be relevant or display a strong correlation to the attractiveness ratings. The mean, second moment, third moment, value for uniformity, value of the texture descriptor R, and the value for entropy displayed good correlation when tested as part of the feature vector. Therefore, these values were used for the final set of values incorporated into the feature vector.

The values shown above effectively describe some of the texture characteristics of a given facial image. The table illustrates significant patterns observed for some of the

texture characteristics observed.

Entropy is a measure of the amount of variability present in an image and is thus a very important measure for the analysis of texture. Entropy helps in assessing the levels of uniformity and variation for a given image. It was observed that an image labeled as unattractive was associated with higher values of entropy and relatively higher values of the texture descriptor R as well.

The texture descriptor R essentially holds the same values as the standard deviation. The standard deviation is a key aspect to observe when taking note of the textural features of an image. This is due to the fact that it is a measure of variability in the intensity levels of the image. Thus, an image with a visibly smoother appearance will have a lower standard deviation than a coarser image, as it will have lesser variability in the intensity levels. This is a major component of the smooth appearance of many images and high intensity values are associated with a greater occurrence of 'smooth' areas on a facial image. It can be concluded that images that appeared to be possessing relatively smooth characteristics obtained higher ratings [53].

Another interesting observation was the correlation between the values for the mean and the attractiveness ratings obtained. Images with higher attractiveness ratings correlate with lower values for the mean.

Figure 23 displays some images and their corresponding attractiveness ratings. The texture feature values corresponding to these ratings can be seen in Table 11.

Figure 23: Images corresponding to the various texture representations and attractiveness levels: top left: attractiveness rating of 5, top center: attractiveness rating of 4, top right: attractiveness rating of 3, bottom left: attractiveness rating of 2, bottom left: attractiveness rating of 1

5.4 Face Shape Analysis

Human faces do not necessarily exhibit geometric shape characteristics, however it has long been observed that human faces falls into five general categories of shape. Most

human faces can be associated with these categories and they include: round, oval, oblong, triangular, and square. Figure 24 helps to illustrate these major shapes.

Current beauty analysis algorithms rarely analyse the overall shape outline of the face. This research has shown that the overall face shape is a key contributor to facial beauty. The shape outline information obtained is a major component of the overall feature vector obtained for final training and testing. The accuracy of the final results decreases by approximately 14% without the use of face shape information.

When observing the any given face, it is the tendency of a human to subconsciously assess the shape of the given face, thus a correlation has been found between how attractiveness is perceived for a given face and its corresponding face shape [53]. In order to formulate an accurate representation for facial attractiveness, it is imperative that this research account for the facial shape characteristics.

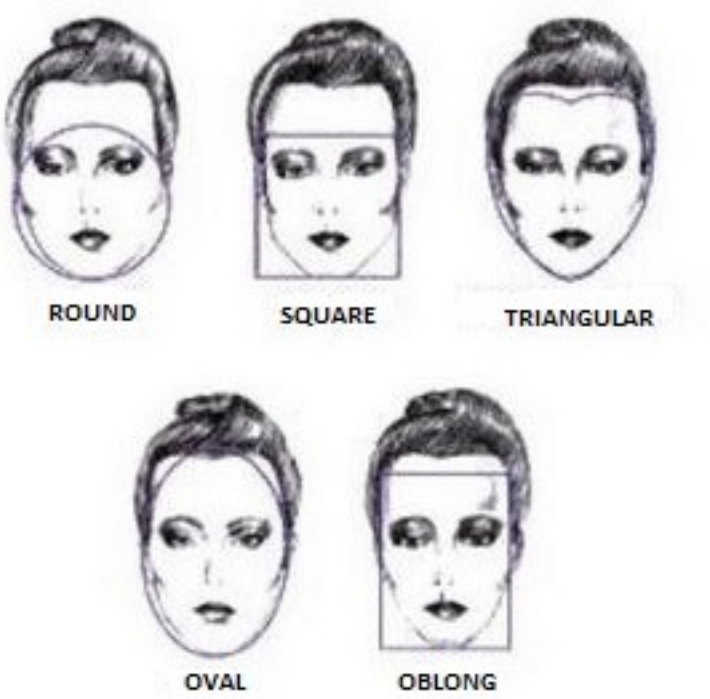

Figure 24: Various face shapes illustrated

The analysis was initially done with images having the resolution of 450 by 350 pixels. Next, the resolution was increased to 800 by 720 for all the feature extraction processes in order to obtain more accurate results. However, the feature extraction for the face shape analysis was not producing very accurate results at this resolution; therefore the resolution was increased to 1200 by 1024 pixels.

The algorithm developed for the analysis of facial shape is based on the concept of Sobel operators. The algorithm improves upon the accuracy of existing Sobel operators by working on innumerous subregions of the face in order to increase accuracy of results obtained. Current research mainly uses Gabor wavelets for edge based feature extraction. The use of Sobel operators for determination of facial shape characteristics is a rather novel approach in the area of facial beauty analysis.

In order to apply the Sobel operator, several masks had to be applied to the various image regions. Initially, only four masks were identified for the operation. These included the masks for the horizontal and vertical orientations in addition to the masks for the two diagonals. The final results were slightly improved when the mask for the non-directional orientation was also included. The following sections help to outline the algorithm formulated for the analysis of facial shape.

5.4.1 Edge Gradient and Face Contour

To help account for the various face shapes, the gradients of the shape outline of the face will be examined as features to be used for training [54]. The method proposed is to build a histogram containing the directions of the gradients of the face edges. This process can then be divided into two sub-modules: detection of the edges and computation of the gradients. Of greater importance is the methodology for computing edge gradient, as this will be a significant feature for training.

The computation of edge gradient is done through Sobel operators. Then, the overall algorithm to compute the set of gradients for the various face regions is presented. It is important to note that the overall face image is divided into small subregions in order to isolate the regions containing the outline of the face shape [55].

Thus, given an image it is divided into subregions of equal size, as can be seen in Figure 25 below. In the case of this image, there is a mask dividing the image into smaller squares that will be processed individually.

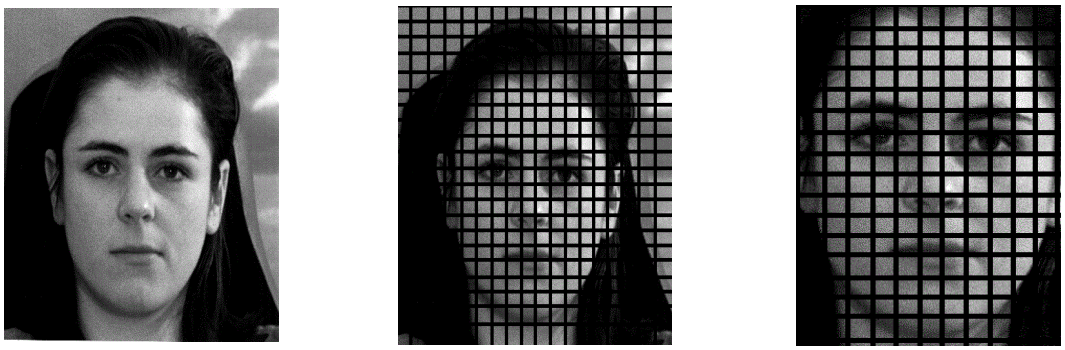

Figure 25: Various steps of dividing the image into subregions

Only the regions along the face contour are then sampled for gradient information. This is a relatively new approach to face beauty analysis as the role of the overall holistic face shape has not been examined in detail before. The edges in the regions along the face shape outline are key aspects for the representation of any face. In order to define the edges of the face, the landmarks detected from the Active Shape Models are used. Thus, the regions of the face containing the points outlining the face are analyzed for gradient information, as seen in Figure 26.

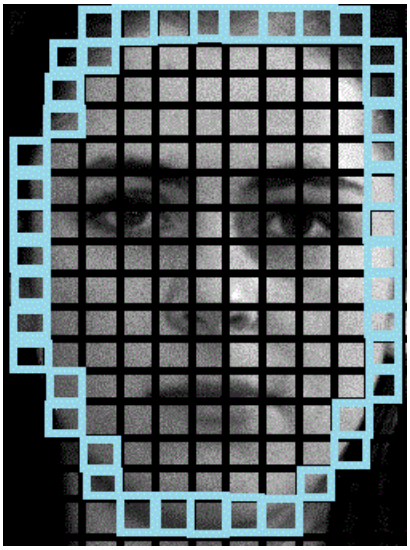

Figure 26: Face shape outline

The algorithm followed to analyse the gradients and hence produce a representation for the overall face outline is as follows:

Input: image, number of vertical and horizontal divisions

For each region:

1. Initialize the filters for 5 different types of edges, these are the Sobel masks

    1(a). Register the size of the image; initialize another matrix of the same size as the image to hold the gradients

2. Apply the Sobel masks through iteration

    2(a). Detect edges

3. Calculate maximum Sobel gradient and value and store these values
4. Save index type of orientation.
5. Multiply each of the various orientations detected by the Sobel masks (convolution)

6. Calculate the histogram for each subimage, eliminate unwanted zeros, and store all into a vector

Output: Vector containing edge gradients for the face outline [55]

This implementation module developed as part of this research was executed in Matlab as image processing functions such as dividing the image into subsections and vector representation of each image are handled very efficiently through Matlab's available libraries.

The five Sobel masks for this implementation essentially represented the 5 various orientations:

1. Vertical
2. Horizontal
3. Diagonals (2 for each orientation of diagonal)
4. Non-directional

The non-directional orientation is used to account for instances when there is no contrast or the orientation is very random.

The Sobel operator helps to compute an approximation of the gradient. After the application of the Sobel operator, each point on an image is represented as its corresponding gradient vector. The Sobel masks are an integral component of the process as the Sobel operator is based on the convolution of the Sobel masks with each image component [55].

The mask matrices used in this research are as follows:

-1	-2	-1	-1	0	+1	+2	+2	-1	-1	+2	+2	-1	0	+1
0	0	0	-2	0	+2	+2	-1	-1	-1	-1	+2	0	0	0
+1	+2	+1	-1	0	+1	-1	-1	-1	1	-1	-1	1	0	-1

Figure 27: Masks for the various orientations: (from left) vertical, horizontal, diagonal1, diagonal2, non-directional)

The convolution of each image subregion with each of these masks produces another matrix equivalent in size with the original image subregion. Convolution is essentially a mathematical operation on two functions which outputs the area overlap between the two functions as a relation of the amount that one of the functions is translated. The convolution process gives the derivatives for the various orientations. The resulting gradient approximations are then combined to give the overall gradient magnitude and direction.

The Sobel operator represents the gradient in a sufficiently accurate quality to be used in this application. Nevertheless, it has several drawbacks as well, which include the fact that intensity values in a very small region are sampled in each iteration, increasing the number of iterations needed for an accurate value [55].

Chapter 6 Experimental Results

Facial beauty is one of the few characteristics that humans often derive happiness from. Naturally, it has long been an area of considerable research in image processing. Having various applications ranging from surgery and facial reconstruction to cosmetics, facial beauty analysis can be used as a stand-alone module in addition to being integrated into larger image processing systems.

This chapter discusses the results obtained from the implementation. The extraction of features is proposed through the identification of landmarks using an algorithm based on the Active Shape Model algorithm. The landmarks are then used for the extraction of geometric, textural, and shape features related to a given face. The sub modules for extracting accurate geometric, textural and shape features are all based on algorithms developed and tested as part of this research. The ratios extracted from the landmarked geometric features were extracted based on an algorithm developed that calculated the distances among the various features. The textural features were extracted based on procedures and modules developed to extract textural information from each image from the database. The shape features were extracted using a Matlab module developed for efficient utilization of the Sobel operator which was an integral part of the shape extraction algorithm.

The algorithms pertaining to the various sub-modules developed have been previously outlined in Chapter 5. The final system developed is outlined below in Figure 28, which shows the significant components and steps followed to establish the system.

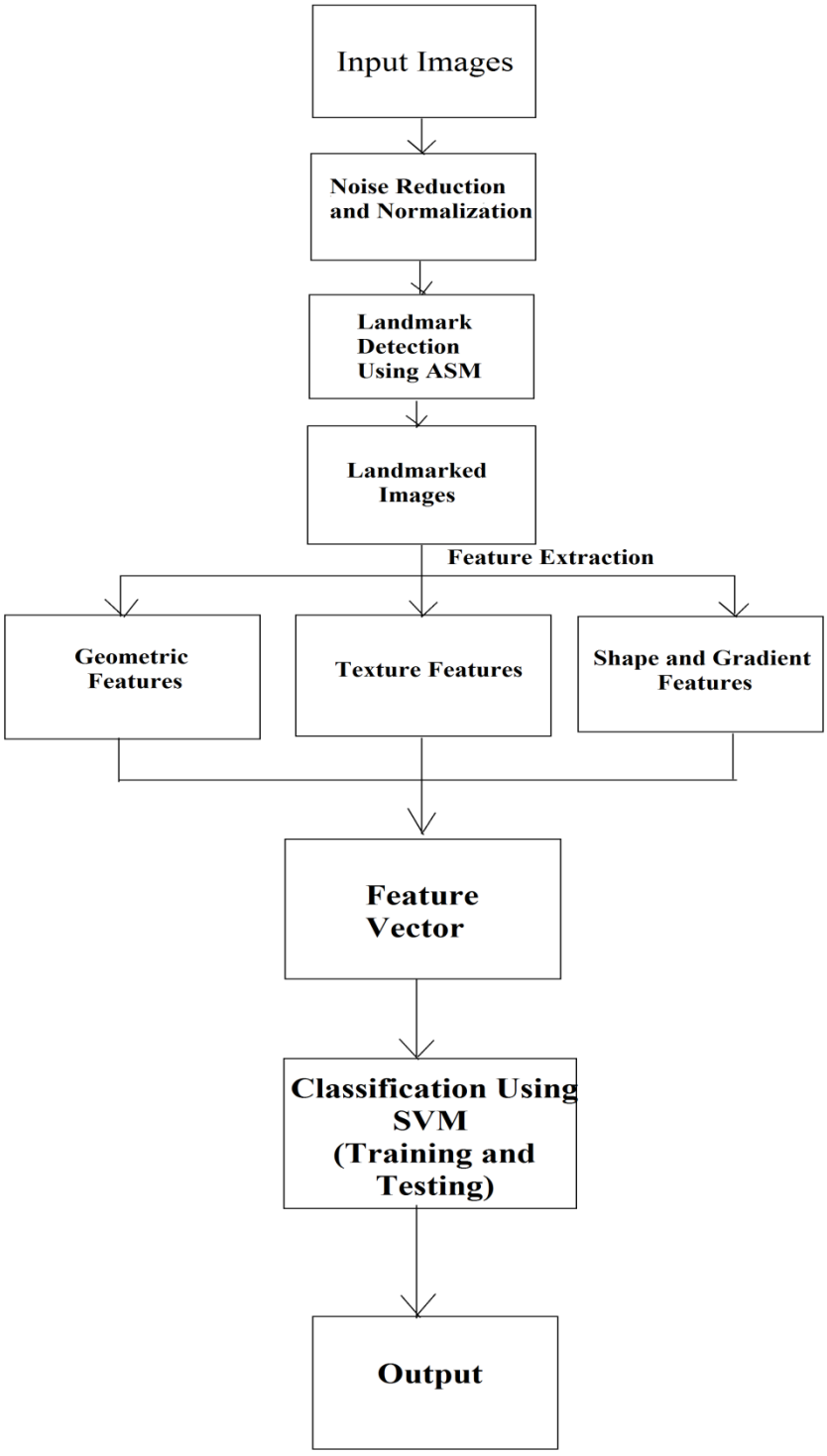

Figure 28: Block Diagram of Beauty Analysis System

Various feature vectors were tested before converging to a vector which produced consistent results. However, in order to plot landmarks and extract these features, the image size needed to be optimum. The results varied according to several key factors, which included the image size and resolution, accuracy of landmark selection, the features selected, and the size of training samples. The final result converged to an accuracy of 85.66 percent.

6.1 Feature Classification

Previous sections of this chapter discuss the various features that are part of the main feature vector used for training. This section will help to outline the results obtained by using Support Vector Machines for the classification of images into the various categories of attractiveness. As mentioned earlier, the five main classes to which an image can be assigned are as follows:

1. Unattractive
2. Below average
3. Average
4. Above average
5. Attractive

6.1.1 Support Vector Machines

Features are necessary to accurately represent a given face as they can quantify the essence of facial beauty. In order to determine how accurate the representation is, the feature vector must be tested through a learning system, which will attempt to learn the

structure of a set of data through training. The learning system is the decision module which will eventually provide the final output.

There are two main types of learning models in machine learning:

- supervised learning
- unsupervised learning

Supervised learning infers patterns from a set of labeled training data, which is made up of a set of training samples. Thus, each piece of training data consists of an input value and its corresponding output value. The supervised learning algorithm then analyzes the training data and produces a function as a result. This function is then used to predict the outputs of further new input data.

Unsupervised learning, on the other hand, attempts to find patterns in unlabeled data and thus there is no error checking mechanism for the evaluation of a potential solution.

The learning methodology utilized in this research is supervised learning, through Support Vector Machines. Support vector machines (SVMs) are supervised learning models that analyze and record patterns which are then used to classify data. A support vector machine does this by building the optimal hyperplane for linearly separable data. The support vectors are the data points that lie closest to the decision surface and have the greatest effect on the ideal location of the decision surface [59].

The best hyperplane for separation of the data is one that has the largest distance to the nearest training data point of a given class, this is known as the functional margin. Larger functional margins usually lead to lowering the generalization error for the classifier. The generalization error essentially measures the ability for a learning machine to generalize to unseen data. This is illustrated in the figure below; as can be seen, three possible

hyperplanes are drawn. The optimum hyperplane, H3, effectively has the largest separation margin.

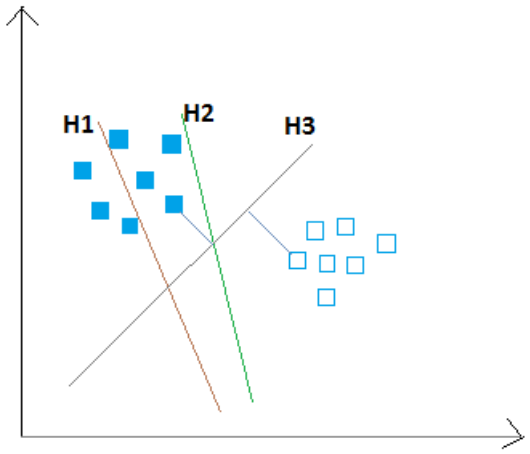

Figure 29: Illustration of possible hyperplanes in a SVM

Thus support vector machines are described as follows:

Given a training set of data, G, which consists of N training points which can be represented as (x_1, y_1), (x_2, y_2), (x_3, y_3) and so on until (x_N, y_N). Here $x_i \epsilon R^n$ and $y_i \epsilon \{-1, 1\}$ in addition to i=1, 2...N.

The objective is to find a set of support vectors; coefficient weights, the constant *b*, and the decision surface such that the distance *d* is maximized. This is illustrated in the figure below. If the data is linearly separable, two hyperplanes can be constructed such that they separate the data with the largest functional margin [60].

The decision factor is represented as shown in Eq. 6.1. The vector *w* defines a direction perpendicular to the hyperplane and is defined as Eq. 6.2 where a_i represents coefficient weights and *b* is a constant.

$$w^T x + b = 0 \tag{6.1}$$

$$W = \sum_{i=1}^{N} a_i y_i x_i \tag{6.2}$$

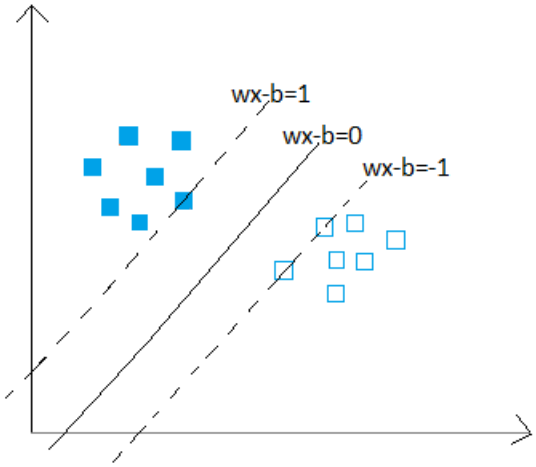

Figure 30: Construction of two main hyperplanes

6.1.1.1 Nonlinear Classification

In the case that the training data, Φ, is not linearly separable, the nonlinearly separable data is mapped into a higher dimensional Euclidean space where data can be linearly separated. This is done through the use of a kernel function, K, where K is defined by Eq. 6.3.

Figure 31 illustrates the mapping of the data into the higher dimension.

$$K(x_i, x_j) = \Phi(x_i), \Phi(x_j) \tag{6.3}$$

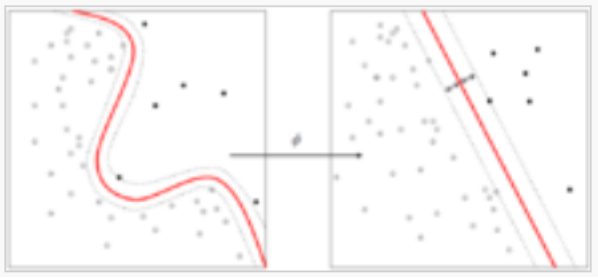

Figure 31: Illustration of mapping to higher dimension in SVM classification

Therefore, when the relationship between the data is nonlinear, there is the use of kernel functions for mapping the data to higher dimensions, where it will display linear patterns. This can be illustrated with the use of an example.

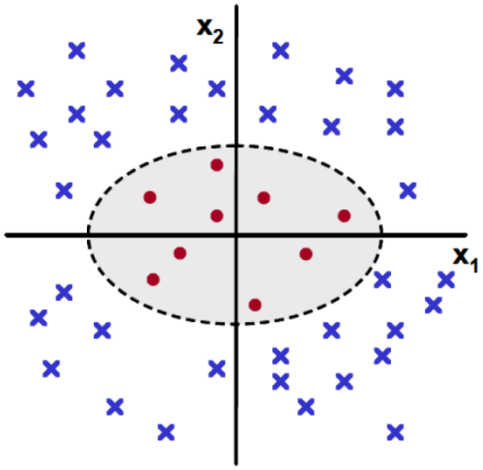

Figure 32: Initial data for illustration of nonlinear classification

Given the data in Figure 32, it can be observed that there is no linear separator existing for this data. Each example here is defined by two features, this can be represented as $x = \{x_1, x_2\}$.

$$x = \{x_1, x_2\} \rightarrow z = x_1^2, \sqrt{2}x_1x_2, x_2^2 \qquad 6.4$$

We can now map each example using the mapping shown in Equation 7.8. Thus, now each data set has three features which are derived from the old representation. Also, now

the data is linearly separable in the new representation. This is illustrated in Figure 33.

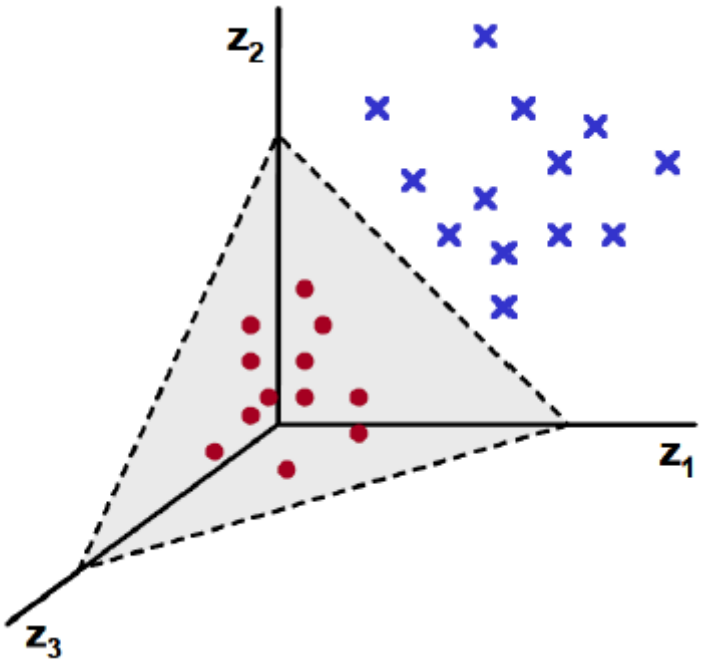

Figure 33: Classified data for nonlinear classification

6.1.1.2 Multiclass Approaches

In the case of the training sets and ground truth data for this research, several classes of data are present. An open source library, LibSVM was used for the implementation of SVM in this research. Thus, when there are three or more classes present, the problem is categorized as a multiclass problem and requires multiclass SVM methods.

The multiclass SVM approach is essentially one of reducing the multiclass classification problem to a binary classification problem by recursively selecting random partitions of the set of classes. Thus, several binary SVM classifiers are used to solve a given multiclass problem [61].

There are three solutions for approaching the multiclass SVM problem. These are

described as follows:

- Ranking SVMs for Multiclass Problems: In this methodology, one SVM decision function is used for the classification of all classes.
- One-Versus-All Method: One binary SVM is constructed to separate members of a given class from members of other classes.
- One-Versus-One: One binary SVM is constructed for pairs of classes in order to separate members of a given class from members of other classes.

The methodology selected for use in this research is the One-Versus-One approach, as the performance was significantly better for this data set and training time was shorter as well. The One-Versus-One approach is based on the max-wins voting strategy, in which the result is obtained by majority vote of all classifiers. In this strategy, every classifier chooses one of two classes to assign, then the vote for the class to which the assignment is made is increased by one. The class with the most votes in the final stage determines the final classification. Therefore, the class that is chosen is the one with votes from the maximal number of pairs of SVMs.

An illustration of the one-versus-one approach for multiclass SVM with three classes is shown in Figure 34. This figure shows the various pair-wise decision boundaries that are constructed for each pair of classes.

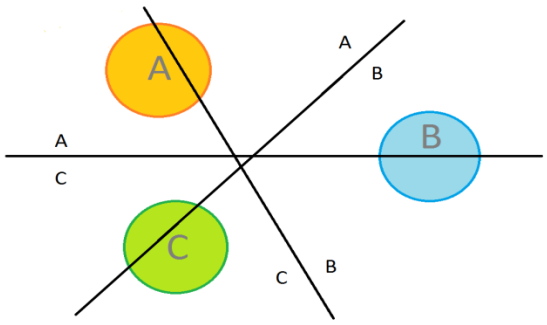

Figure 34: Illustration of one-versus-one approach for multiclass SVM

In this research, various kernel functions were experimented with. The various kernels that were used include: polynomial, radial basis function (RBF), and sigmoid. The SVM was eventually configured with only the parameters from the radial basis function as that generated the best results when compared with those of other kernel functions. Thus, the RBF is used to map the data sets into a higher sample space. The RBF kernel is represented by the equation below:

$$K(X_i, X_j) = \exp(-\gamma \|X_i - X_j\|^2)$$

Using the various kernel functions, the results of testing are shown in Table 12 below.

Kernel Function	**Results on Training Database (215 images)**	**Results on Testing Database (100 images)**
Polynomial	74.20%	70.50%
Radial Basis Function (RBF)	85.66%	80.00%
Sigmoid	78.30%	75.50%

Table 12: Results Achieved for each SVM Kernel Function

6.2 Correlations in Results

The correlations between the size of the various facial features for a particular image and

the corresponding attractiveness ratings was analysed as part of the results analysis. In order to do this, the mean physical attractiveness rating for each target image was found, and the correlation between the size of a particular feature and the average ratings was found.

Feature	Complete Sample (n =215)
Eye Height	0.68
Eye Width	0.71
Iris Width	0.35
Separation of Eyes	0.12
Nose Tip Width	-0.10
Nostril Width	0.45
Nose Length	-0.02
Nose Area	-0.31
Upper Lip Thickness	0.10
Lower Lip Thickness	0.76
Chin Length	-0.21
Cheekbone Width	0.86
Cheek Width	0.39
Mid-face Length	0.01
Eyebrow Height	0.79
Pupil Width	0.68
Standardized Pupil Width	0.30
Smile Height	0.54
Smile Width	0.38

Table 13: Correlations of Feature Measurements with Attractiveness Ratings

The facial features examined are based on theories of facial attractiveness that will be discussed in other chapters. The correlation methodology used was the Pearson product moment correlation which is one of the most commonly used correlation coefficients. The measurements corresponding to each facial feature were obtained by running a set of algorithms on the set of images. Table 13 outlines the correlation results that were

obtained for major facial features.

Correlation values lie between 1 and -1. A value of 0 indicates no association between the two variables or items. A value greater than 0 indicates a positive association and a value lesser than 0 indicates a negative association between the given values. A positive association essentially means that as one variable increases, the other variable increases as well. A negative correlation implies that as one variable increases the other variable tends to decrease. The measurements displayed in the table help to illustrate a set from the overall set of features extracted. The features are displayed due to their weight in the final feature vector and the extent of influence they have on the accuracy of results.

6.3 Training Database

As described in Chapter 3, a total of seven databases were used to source the images that were used for the purposes of this research. From these databases, various images were selected according how well the particular image would fit the research criteria. The criteria included that the images should be of female participants and that the images should not have any ornamentation such as earrings, hair accessories, etc. Chapter 3 elaborates further on the details associated with the number of images taken from each database.

The final training database consisted of 215 images with a total of 65 features being part of the final feature vector. These images were part of the various databases discussed in Section 3.1 of Chapter 3. The training database consisted of images with well distributed attractiveness ratings.

When referring to the number that is attributed to the attractiveness ratings, we are

referring to the scale that was used for the attractiveness ratings survey. The survey utilized a scale which ranged from 1 to 5, with 1 corresponding to a rating of "unattractive", 2 corresponding to a rating of "below average", 3 corresponding to a rating of "average", 4 corresponding to a rating of "above average" and 5 corresponding to a rating of "attractive", which corresponds to the attractiveness of the individual in the image being described as "average".

Among the images used for training, 68 of the images had been assigned an average attractiveness rating of 3. A total of 17 images with the attractiveness rating of 1 were further selected and a total of 50 images with the rating of 2 were selected. There were also 58 images with a rating of 4, and 22 images with an average attractiveness rating of 5. The distribution and corresponding numbers are outlined in Figure 35. The attractiveness ratings from the survey conducted previously were used as the ground truth data for the database.

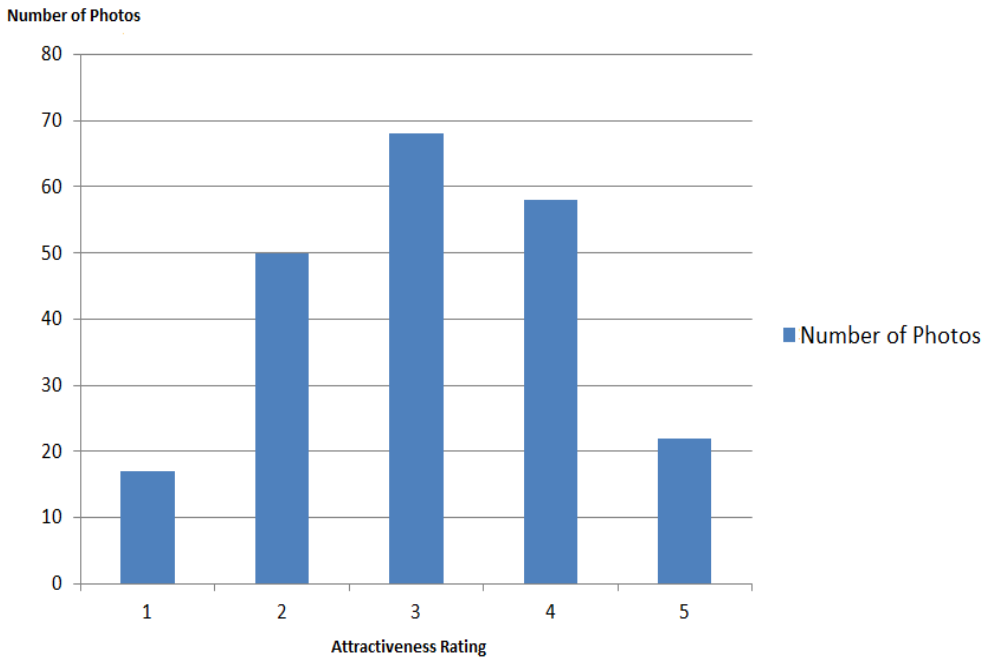

Figure 35: Number of Images in Training Database Corresponding to each Rating

6.4 Testing Database

A total of 100 images were used for the testing process. The feature vector is extracted for the given set of images that were part of the testing database. The vector is then classified into one of the five attractiveness classes. In addition, Figure 36 summarizes the number of images corresponding to each attractiveness rating.

During the testing phase, several variations of the feature vector were experimented with in order to result in a vector with the optimum features for representing the human face accurately. In the case of geometric features, there was considerable difficulty in finding the right mix of features for resulting in the highest accuracy. There were a great number of combinations and going through all the combinations manually was painstaking,

therefore a quick method was determined to permute through the various combinations of geometric features from each set.

The next set of features included the textural features, which were made up of three main groups. This included spectral, statistical and structural textural features. It was important to isolate the category of features that best applied for the representation of the human face. Through several tests and experimentation, it was determined that the statistical textural features were best suited for the purposes of this research.

The final set of features used included features for edge orientation information; this set of features was used mainly to represent the overall face shape and outline. This was a set of features of considerable importance as the overall face shape is known to be a deciding factor when it comes to measuring attractiveness levels in a given human face. However, there was an error that was occurring from the measurement taken from the area near the chin. The features being extracted from the chin and the nearby region were not being accurately represented. Therefore, it was decided that this region will be broken down into more parts than what was applied to the rest of the face. This means to say that although the outline of the face was being broken down into small squares for the extraction of edge information, the area near the chin would have the squares broken down further into small component squares. This iterative approach helped to gain more accurate face shape and edge outline information.

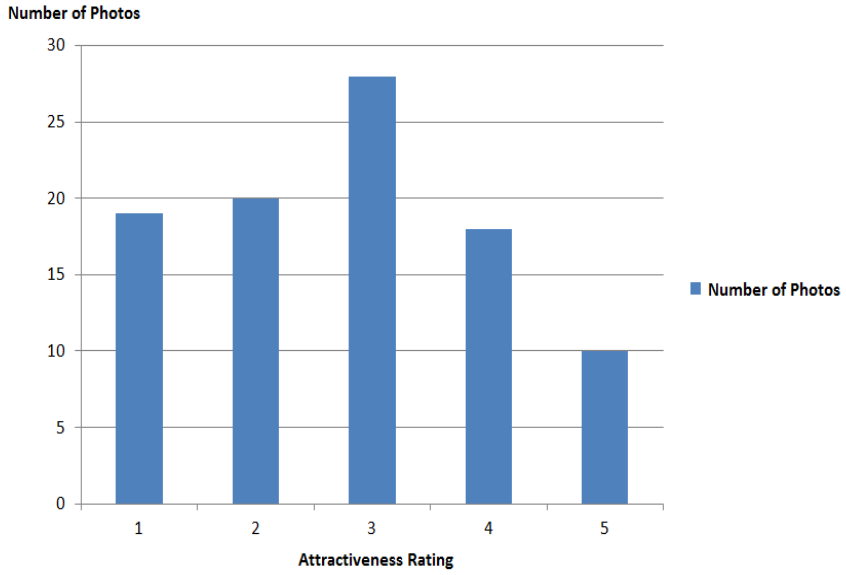

Figure 36: Number of Images in Testing Database Corresponding to each Rating

6.5 Values Utilized

The experimental results were obtained with the variation of values chosen for C and γ. These approximate values were obtained through cross validation and a parse grid search, in which the available data are split into a given number of subsets. The cross validation error is then computed for various values for C and γ. Finally, the C and γ with the lowest cross validation error is chosen for use on the training data set.

After obtaining an approximation for values of C and γ, adjustments were made to the values in order to improve the performance results. The values of C and γ that were found to have the highest classification rates were C=0.0625 and γ = 0.00390625.

Shown in Figure 37 are some images that were wrongly classified during the testing process. It could be hypothesized that the reason why these images were incorrectly classified was because the face had slight amounts of hair covering the outline of the

face. One of the images also has the hair slightly covering an eyebrow; this could have possibly led to discrepancies. These factors thus resulted in inaccurate feature representations which in turn led to incorrect classification. The next chapter focuses mainly on examples of cases that were observed during the research. It presents particular cases and provides a detailed description of the features associated with them. This aims to help illustrate the spectrum of attractiveness through a few chosen images and their respective characteristic features.

Figure 37: Samples of incorrectly classified images

Chapter 7 Illustrative Examples

This thesis aims to present an automatic system for the analysis of female facial beauty. The efforts have been concentrated around developing an accurate representation of the aesthetic aspects of the human face. This representation was then utilized for the purposes of analyzing each image. The analysis aided in the evaluation of an attractiveness rating for the given image. The attractiveness spectrum ranged from “unattractive” to “attractive”, with ratings of 1 and 5 respectively. All images were normalized prior to feature extraction and testing.

To help illustrate the values associated with each attractiveness level, a few examples are presented below. For each example, a detailed description is given of the various features that were extracted for all the various aspects which include the geometric aspects, the textural aspects, and the facial shape aspects. For each feature group, the actual results obtained are given in detail. This thus aims to present a subset of the actual set of results finally obtained. The values included in the table are representative of the final feature vector used for training, the features shown below were particularly chosen because they had great weight in the final feature vector and contributed greatly to the accuracy while testing.

7.1 Attractiveness Level 1

Figure 38: Image with attractiveness rating of 1

7.1.1 Geometric Features

Table 14 shows the values obtained for the geometric features for the given image in Figure 38. This image received an overall attractiveness rating of 1. The geometric representation takes into consideration various theories of facial geometry, which include the Facial Thirds method and the Golden Ratio. Applying these theories helps create an accurate representation of the human face. The table below shows the values obtained for several of the ratios that were calculated for the final feature vector. For each image, the

landmarks were initially detected directly on the image itself, and then the map of labeled points was scaled to a coordinate system. Finally, an automatic computer application was programmed to compute each of the measurements associated with the geometric feature vector.

Measurement ID	Description	Value for Measurement(cm)
1	Vertical distance between top of forehead and chin	4.22
2	Horizontal distance between outer edges of cheekbones	3.73
3	Horizontal distance between outer cheeks at the mouth	2.14
4	Vertical distance between eyebrow and hair	1.45
5	Vertical length of upper head including hair (not shown)	5.79
6	Vertical distance between pupil center and eyebrow	1.21
7	Vertical distance between upper and lower edge of eye	0.59
8	Horizontal distance between inner corner and outer corner of the eye	1.78
9	Horizontal width of iris	0.39
10	Horizontal distance between centre of pupils	3.84
11	Diagonal distance between left eye and center of the mouth	3.11
12	Diagonal distance between right eye and center of the mouth	3.1

Table 14: Values of sample geometric measurements

7.1.2 Textural Features

Table 15 displays a sample of the textural results that was obtained for the image shown in Figure 38. These values shown are typical ones obtained for many other images in the same attractiveness category as this image. The values of the third moment, R, and

Entropy are the highest in comparison with the images that received a higher attractiveness rating; this is mostly due to the presence of greater levels of variation in the image.

Mean	Third Moment	R(normalized)	Entropy
197.34	84.14	0.08	8.18

Table 15: Values of sample textural features

7.1.3 Facial Shape Features

The facial shape obtained for this particular image was square. This overall face shape was determined through the face shape analysis done through the Sobel filters and masks. In the scope of this research, the square face shape was observed to be less likely to be associated with a very high attractiveness rating.

7.2 Attractiveness Level 2

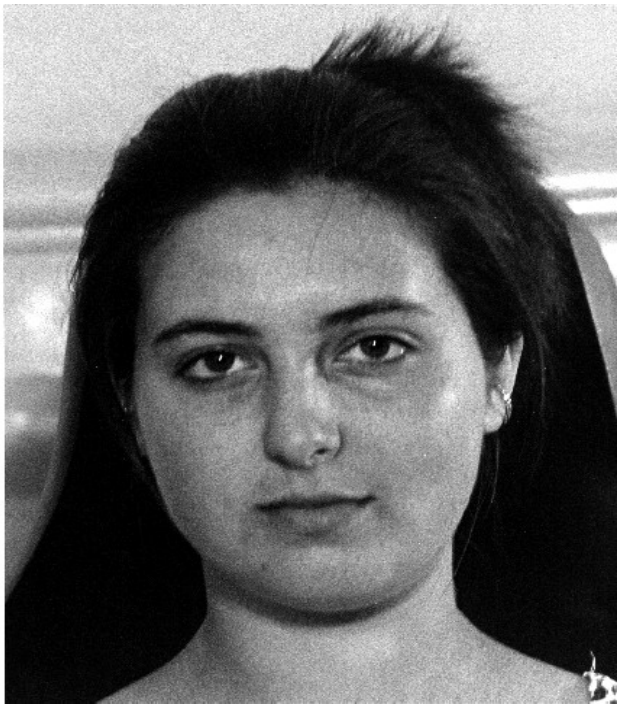

Figure 39: Image with attractiveness rating of 2

7.2.1 Geometric Features

Table 16 shows the values obtained for the geometric features for the given image in Figure 39. This image received an overall attractiveness rating of 2.

Measurement ID	Description	Value for Measurement(cm)
1	Vertical distance between top of forehead and chin	5.17
2	Horizontal distance between outer edges of cheekbones	3.69
3	Horizontal distance between outer cheeks at the mouth	2.25
4	Vertical distance between eyebrow and hair	1.57
5	Vertical length of upper head including hair (not shown)	6.1
6	Vertical distance between pupil center and eyebrow	1.17
7	Vertical distance between upper and lower edge of eye	0.61
8	Horizontal distance between inner corner and outer corner of the eye	1.71
9	Horizontal width of iris	0.43
10	Horizontal distance between centre of pupils	3.89
11	Diagonal distance between left eye and center of the mouth	3.15
12	Diagonal distance between right eye and center of the mouth	3.13

Table 16: Values of sample geometric measurements

7.2.2 Textural Features

Table 17 displays a sample of the textural results that was obtained for the image shown in Figure 39. These are typical values obtained for many other images in the same attractiveness category as this image. The values of the third moment, R, and Entropy are the second highest in comparison with the images that received a higher attractiveness rating. This is mostly due to the presence of greater levels of variation in the image.

Mean	Third Moment	R(normalized)	Entropy
165.74	58.12	0.07	6.97

Table 17: Values of sample textural features

7.2.3 Facial Shape Features

The facial shape obtained for this particular image was round. This overall face shape was determined through the face shape analysis done through the Sobel filters and masks. The round face shape was observed to be more likely to be associated with a very high attractiveness rating. This might be due to the more symmetrical characteristics associated with this face shape.

7.3 Attractiveness Level 3

Figure 40: Sample image with attractiveness rating of 3

7.3.1 Geometric Features

Table 18 shows the values obtained for the geometric features for the given image in

Figure 40. This image received an overall attractiveness rating of 3. The geometric representation takes into consideration various theories of facial geometry, which include the Facial Thirds method and the Golden Ratio.

Measurement ID	Description	Value for Measurement(cm)
1	Vertical distance between top of forehead and chin	4.89
2	Horizontal distance between outer edges of cheekbones	3.62
3	Horizontal distance between outer cheeks at the mouth	2.17
4	Vertical distance between eyebrow and hair	1.46
5	Vertical length of upper head including hair (not shown)	6.12
6	Vertical distance between pupil center and eyebrow	1.11
7	Vertical distance between upper and lower edge of eye	0.68
8	Horizontal distance between inner corner and outer corner of the eye	1.65
9	Horizontal width of iris	0.41
10	Horizontal distance between centre of pupils	3.81
11	Diagonal distance between left eye and center of the mouth	3.19
12	Diagonal distance between right eye and center of the mouth	3.11

Table 18: Values of sample geometric measurements

7.3.2 Textural Features

Table 19 displays a sample of the textural results that was obtained for the image shown in Figure 40. These values shown are typical of values obtained for many other images in

the same attractiveness category as this image. The values of the third moment, R, and Entropy are the generally high in comparison with the images that received a higher attractiveness rating. This is mostly due to the presence of greater levels of variation in the image.

Mean	Third Moment	R(normalized)	Entropy
121.14	50.73	0.04	6.51

Table 19: Values of sample textural features

7.3.3 Facial Shape Features

The facial shape obtained for this particular image was round. This overall face shape was determined through the face shape analysis done through the Sobel filters and masks. The round face shape was observed to be more likely to be associated with a very high attractiveness rating. This might be due to the more symmetrical characteristics associated with this face shape.

7.4 Attractiveness Level 4

Figure 41: Sample image with attractiveness rating of 4

7.4.1 Geometric Features

Table 20 shows the values obtained for the geometric features for the given image in Figure 41. This image received an overall attractiveness rating of 4. The geometric representation takes into consideration various theories of facial geometry, which include the Facial Thirds method and the Golden Ratio.

Measurement ID	Description	Value for Measurement(cm)
1	Vertical distance between top of forehead and chin	5.12
2	Horizontal distance between outer edges of cheekbones	3.86
3	Horizontal distance between outer cheeks at the mouth	2.25
4	Vertical distance between eyebrow and hair	1.53
5	Vertical length of upper head including hair (not shown)	6.19
6	Vertical distance between pupil center and eyebrow	1.16
7	Vertical distance between upper and lower edge of eye	0.73
8	Horizontal distance between inner corner and outer corner of the eye	1.82
9	Horizontal width of iris	0.57
10	Horizontal distance between centre of pupils	3.86
11	Diagonal distance between left eye and center of the mouth	3.21
12	Diagonal distance between right eye and center of the mouth	3.13

Table 20: Values of sample geometric measurements

7.4.2 Textural Features

Table 21 displays a sample of the textural results that was obtained for the image shown in Figure 41. These values shown are typical of values obtained for many other images in the same attractiveness category as this image. The values of the third moment, R, and Entropy are the generally lower in comparison with the images that received higher attractiveness ratings. This is mostly due to the presence of lower levels of variation in the image.

Mean	Third Moment	R(normalized)	Entropy
109.15	34.62	0.03	5.35

Table 21: Values of sample textural features

The high attractiveness rating could be associated with the ideal textural feature values, this could be explained by the fact that theoretically faces with smoother textures are often found to be more attractive.

7.4.3 Facial Shape Features

The facial shape obtained for this particular image was oval. This overall face shape was determined through the face shape analysis done through the Sobel filters and masks. The oval face shape was observed to be most likely to be associated with a very high attractiveness rating. This might be due to the symmetrical characteristics associated with this face shape.

7.5 Attractiveness Level 5

Figure 42: Sample image with attractiveness rating of 5

7.5.1 Geometric Features

Table 22 shows the values obtained for the geometric features for the given image in Figure 42. This image received an overall attractiveness rating of 5. The geometric representation takes into consideration various theories of facial geometry, which include the Facial Thirds method and the Golden Ratio.

Measurement ID	Description	Value for Measurement(cm)
1	Vertical distance between top of forehead and chin	5.25
2	Horizontal distance between outer edges of cheekbones	3.83
3	Horizontal distance between outer cheeks at the mouth	2.26
4	Vertical distance between eyebrow and hair	1.51
5	Vertical length of upper head including hair (not shown)	5.98
6	Vertical distance between pupil center and eyebrow	1.24
7	Vertical distance between upper and lower edge of eye	0.59
8	Horizontal distance between inner corner and outer corner of the eye	1.61
9	Horizontal width of iris	0.52
10	Horizontal distance between centre of pupils	3.62
11	Diagonal distance between left eye and center of the mouth	3.35
12	Diagonal distance between right eye and center of the mouth	3.11

Table 22: Values of sample geometric measurements

7.5.2 Textural Features

Table 23 displays a sample of the textural results that was obtained for the image shown in Figure 42. These values shown are typical of values obtained for many other images in the same attractiveness category as this image. The values of the third moment, R, and Entropy are the generally lowest in comparison with the images that received a higher attractiveness rating. This is mostly due to the presence of the lowest levels of variation in the image.

Mean	Third Moment	R(normalized)	Entropy
88.12	29.18	0.01	4.08

Table 23: Values of sample textural features

7.5.3 Facial Shape Features

The facial shape obtained for this particular image was oval. This overall face shape was determined through the face shape analysis done through the Sobel filters and masks. The oval face shape was observed to be most likely to be associated with a very high attractiveness rating. This might be due to the symmetrical characteristics associated with this face shape.

7.6 Miss World 2010

Figure 43: Image of Miss World 2010

7.6.1 Geometric Features

This research also contained images of various beauty pageant contestants and this section aims to show the results associated with one such image. Table 24 shows the values obtained for the geometric features for the given image in Figure 43. The image in Figure 43 is of Miss World 2010, Alexandria Mills. This image received an overall attractiveness rating of 4. The geometric representation takes into consideration various theories of facial geometry, which include the Facial Thirds method and the Golden Ratio.

Being a beauty pageant winner, Mills has some feature measurements that are definitely outstanding, these include the following measurements:

- Horizontal distance between outer edges of cheekbones
- Vertical distance between pupil center and eyebrow
- Horizontal distance between inner corner and outer corner of the eye

Measurement ID	Description	Value for Measurement(cm)
1	Vertical distance between top of forehead and chin	5.67
2	Horizontal distance between outer edges of cheekbones	4.12
3	Horizontal distance between outer cheeks at the mouth	2.19
4	Vertical distance between eyebrow and hair	1.62
5	Vertical length of upper head including hair (not shown)	5.71
6	Vertical distance between pupil center and eyebrow	1.52
7	Vertical distance between upper and lower edge of eye	0.59
8	Horizontal distance between inner corner and outer corner of the eye	1.72
9	Horizontal width of iris	0.33
10	Horizontal distance between centre of pupils	3.82
11	Diagonal distance between left eye and center of the mouth	3.58
12	Diagonal distance between right eye and center of the mouth	3.41

Table 24: Values of sample geometric measurements

7.6.2 Textural Features

Table 25 displays a sample of the textural results that was obtained for the image shown in Figure 43. These values shown are typical of values obtained for many other images in the same attractiveness category as this image. The values of the third moment, R, and Entropy are the generally lowest in comparison with the images that received a higher

attractiveness rating; this is mostly due to the presence of the lowest levels of variation in the image.

Mean	Third Moment	R(normalized)	Entropy
97.12	31.18	0.01	4.01

Table 25: Values of sample textural features

7.6.3 Facial Shape Features

The facial shape obtained for this particular image was oval. This overall face shape was determined through the face shape analysis done through the Sobel filters and masks. The oval face shape was observed to be most likely to be associated with a very high attractiveness rating. This might be due to the symmetrical characteristics associated with this face shape.

7.7 Miss Universe 2010

Figure 44: Image of Miss Universe 2010

7.7.1 Geometric Features

This research also contained images of various beauty pageant contestants and this section aims to show the results associated with one such image. Table 26 shows the values obtained for the geometric features for the given image in Figure 44. The image in Figure 44 is of Jimena Navarrete, who was crowned Miss Universe 2010. This image received an overall attractiveness rating of 5. The geometric representation takes into consideration various theories of facial geometry, which include the Facial Thirds method and the Golden Ratio.

Several feature measurements also stand out for Jimena. These are as follows:

- Horizontal distance between centers of pupils
- Diagonal distance between left eye and center of the mouth
- Diagonal distance between right eye and center of the mouth

- Vertical distance between top of forehead and chin

Measurement ID	Description	Value for Measurement(cm)
1	Vertical distance between top of forehead and chin	5.74
2	Horizontal distance between outer edges of cheekbones	3.79
3	Horizontal distance between outer cheeks at the mouth	1.81
4	Vertical distance between eyebrow and hair	1.71
5	Vertical length of upper head including hair (not shown)	5.81
6	Vertical distance between pupil center and eyebrow	1.17
7	Vertical distance between upper and lower edge of eye	0.69
8	Horizontal distance between inner corner and outer corner of the eye	1.41
9	Horizontal width of iris	0.42
10	Horizontal distance between centers of pupils	3.79
11	Diagonal distance between left eye and center of the mouth	3.60
12	Diagonal distance between right eye and center of the mouth	3.39

Table 26: Values of sample geometric measurements

7.7.2 Textural Features

Table 27 displays a sample of the textural results that was obtained for the image shown in Figure 44. These values shown are typical of values obtained for many other images in the same attractiveness category as this image. The values of the third moment, R, and Entropy are the generally lowest in comparison with the images that received a higher attractiveness rating. This is mostly due to the presence of the lowest levels of variation in the image.

Mean	Third Moment	R(normalized)	Entropy
93.15	31.17	0.01	4.80

Table 27: Values of sample textural features

7.7.3 Facial Shape Features

The facial shape obtained for this particular image was round. This overall face shape was determined through the face shape analysis done through the Sobel filters and masks. The round face shape was observed to be more likely to be associated with a very high attractiveness rating. This might be due to the more symmetrical characteristics associated with this face shape.

7.8 Elizabeth Taylor

Figure 45: Image of Elizabeth Taylor

7.8.1 Geometric Features

To help illustrate various levels of attractiveness, images of attractive actresses were analyzed as part of this research. Table 28 shows the values obtained for the geometric features for the given image in Figure 45. The image in Figure 45 is of Elizabeth Taylor, who is a famous actress. This image received an overall attractiveness rating of 5. The geometric representation takes into consideration various theories of facial geometry, which include the Facial Thirds method and the Golden Ratio.

Several feature measurements also stand out for Elizabeth Taylor. These are as follows:

- Horizontal distance between centers of pupils
- Diagonal distance between left eye and center of the mouth
- Diagonal distance between right eye and center of the mouth
- Vertical distance between top of forehead and chin

Measurement ID	Description	Value for Measurement(cm)
1	Vertical distance between top of forehead and chin	5.79
2	Horizontal distance between outer edges of cheekbones	3.85
3	Horizontal distance between outer cheeks at the mouth	2.23
4	Vertical distance between eyebrow and hair	1.82
5	Vertical length of upper head including hair (not shown)	5.89
6	Vertical distance between pupil center and eyebrow	1.24
7	Vertical distance between upper and lower edge of eye	0.69
8	Horizontal distance between inner corner and outer corner of the eye	1.43
9	Horizontal width of iris	0.42
10	Horizontal distance between centre of pupils	3.82
11	Diagonal distance between left eye and center of the mouth	3.51
12	Diagonal distance between right eye and center of the mouth	3.20

Table 28: Values of sample geometric measurements

7.7.2 Textural Features

Table 29 displays a sample of the textural results that was obtained for the image shown in Figure 45. These values shown are typical of values obtained for many other images in the same attractiveness category as this image. The values of the third moment, R, and Entropy are the generally lowest in comparison with the images that received a higher attractiveness rating; this is mostly due to the presence of the lowest levels of variation in the image.

Mean	Third Moment	R(normalized)	Entropy
81.14	22.10	0.01	3.03

Table 29: Values of sample textural features

The mean values associated with this image are typical of those of images with high attractiveness ratings. The third moment is observed to have one of the lowest values observed in the scope of this research. The entropy has a low value as well because of lower levels of variation.

7.7.3 Facial Shape Features

The facial shape obtained for this particular image was round. This overall face shape was determined through the face shape analysis done through the Sobel filters and masks. The round face shape was observed to be more likely to be associated with a very high attractiveness rating. This might be due to the more symmetrical characteristics associated with this face shape.

7.9 Marilyn Monroe

Figure 46: Image of Marilyn Monroe

7.9.1 Geometric Features

To help illustrate various levels of attractiveness, images of attractive actresses were analyzed as part of this research. Table 30 shows the values obtained for the geometric features for the given image in Figure 46. The image in Figure 46 is of Marilyn Monroe, who is a famous actress. This image received an overall attractiveness rating of 5. The geometric representation takes into consideration various theories of facial geometry, which include the Facial Thirds method and the Golden Ratio.

Several feature measurements also stand out for Marilyn Monroe. These are as follows:

- Horizontal distance between centers of pupils
- Diagonal distance between left eye and center of the mouth
- Diagonal distance between right eye and center of the mouth

- Vertical distance between top of forehead and chin
- Horizontal width of iris
- Vertical distance between eyebrow and hair
- Horizontal distance between outer edges of cheekbones

Measurement ID	Description	Value for Measurement(cm)
1	Vertical distance between top of forehead and chin	5.82
2	Horizontal distance between outer edges of cheekbones	3.91
3	Horizontal distance between outer cheeks at the mouth	2.20
4	Vertical distance between eyebrow and hair	1.71
5	Vertical length of upper head including hair (not shown)	5.93
6	Vertical distance between pupil center and eyebrow	1.29
7	Vertical distance between upper and lower edge of eye	0.51
8	Horizontal distance between inner corner and outer corner of the eye	1.41
9	Horizontal width of iris	0.91
10	Horizontal distance between centre of pupils	3.61
11	Diagonal distance between left eye and center of the mouth	3.39
12	Diagonal distance between right eye and center of the mouth	3.11

Table 30: Values of sample geometric measurements

7.9.2 Textural Features

Table 31 displays a sample of the textural results that was obtained for the image shown in Figure 46. These values shown are typical of values obtained for many other images in the same attractiveness category as this image. The values of the third moment, R, and

Entropy are the generally lowest in comparison with the images that received a higher attractiveness rating; this is mostly due to the presence of the lowest levels of variation in the image.

Mean	Third Moment	R(normalized)	Entropy
80.12	20.17	0.01	4.05

Table 31: Values of sample textural features

The mean values associated with this image are typical of those of images with high attractiveness ratings. The mean is quite low indicating a good intensity distribution. The entropy has a low value as well because of lower levels of variation. The value of R is one of the lowest observed so far in the scope of this research.

7.9.3 Facial Shape Features

The facial shape obtained for this particular image was oval. This overall face shape was determined through the face shape analysis done through the Sobel filters and masks. The round face shape was observed to be most likely to be associated with a very high attractiveness rating. This might be due to the most symmetrical characteristics associated with this face shape.

Chapter 8 Conclusions and Future Work

This thesis has focused on the development of an automatic system for the analysis of human facial beauty. This is done through the analysis of a given facial image and the subsequent assignment of an attractiveness level to the particular image.

8.1 Conclusions

The data sets used for this research were sourced from various publicly available data sets that are often used for research in image processing. These sets also included images from a diverse and eclectic group of women, with varying levels of attractiveness. There were a total of 215 images used for the purposes of this research. In order to establish the ground truths for this research, an experimental survey was conducted. A diverse group of 48 participants agreed to take part in the research. The survey consisted of the participants individually rating each image in the data sets to indicate their personal rating of the attractiveness of the female in the image. These ratings were then analysed for consistencies throughout the various individuals in order to assure the accuracy of representation of the ratings. It was found that there were strong correlations and consistencies within the ratings and this thus established to a great extent the accuracy of the ratings.

The automatic facial beauty analysis system consisted of two main components; the first part of which included the feature extraction and analysis of the given photograph and the second part consisted of the training and testing of the machine learning system that would be used for the prediction of attractiveness levels of any given image. Feature selection was an integral constituent of the system as this determines that accuracy with

which any given image is represented. Therefore, the feature selection process had to make sure the vital aspects related to beauty analysis were well represented in the algorithm used for the identification of facial beauty.

The final feature vector converged to a set that consisted of features related to the key aspects of human facial beauty, these included geometric features, textural features and edge contour features as well. Another integral component of this research was the application of active shape models for the accurate localization of facial features. This was a novel approach in the area of facial beauty analysis as previous research has often faced the difficulties of being able to accurately recognize key facial landmarks. Through the use of active shape models, the accuracy of results was greatly improved to lead towards an overall result of around 86%. The 14% were classified incorrectly mainly due to various facial features being not fully incorporated into the facial representation due to being blocked by hair. In addition, in various instances the hair obstructs the formation of a clear facial outline.

8.2 Future Work

This research has aimed to provide a methodology for the analysis of human facial beauty. This has been accomplished through incorporating various features for the representation of facial beauty as well as making use of the machine learning techniques that provide the most reliable and accurate results. There are, however, several future additions that can be done to further the work already presented. A brief description of these is as follows:

1. Incorporation of New Beauty Models: Several models have been carefully chosen

and represented in this research; these models were based on studies conducted in the areas of aesthetics, sociology, and anthropology. However, the models can be improved if the psychological aspect of human beauty is also taken into consideration. Therefore, future work can also help to account for psychological models of human facial beauty.

2. Incorporate Models for Various Cultures: This research has tried its best to include images and respondents from all various cultures as possible. However, there are several ethnicities that have not been represented in this research, which include ethnicities from various regions of Africa. Future work could focus on the addition of these ethnicities as well.
3. Addition of Methodology for Male Attractiveness: This research has focused on only the attractiveness levels associated with females. However, of great interest are also the attractiveness ratings associated with males. A possible focus of future research could be models associated to human male attractiveness.

REFERENCES

[1] "Pots of Promise." *The Economist* 22 May 2003, http://www.economist.com/node/1795852, retrieved 10 October 2012.

[2] Kringelbach, Morten, "The Human Orbitofrontal Cortex: Linking Reward to Hedonic Experience," Nature, Vol 6.1, (2005):691-673.

[3] AARABI, P., HUGHES, D., The automatic measurement of facial beauty, 2001 IEEE International Conference on Systems, Man, and Cybernetics, Vol 12A, Page(s): 2644 -2647, 2001.

[4] John, Kirkland. "Categorical Perception of Facial Expressions of Emotion: Evidence from Multidimensional Scaling." *Cognition and Emotion,* Vol 3, Page(s): 112-142, 2001.

[5] Ying-Li,Tian, Takeo Kanade, "Recognizing Action Units for Facial Expression Analysis," *IEEE Transactions on Pattern Analysis and Machine Intelligence,* Vol 23.2, Page(s) 454-473, (2001).

[6] Kalkofen et al. "Kant's "Facial Aesthetics" and Galton's "Composite Portraiture" – Are Prototypes beautiful?" *Proceedings of the Xlth International Colloquium on Empirical Aesthetics*, Pages 23-45, 1990.

[7] Smithson, Craig. " Francis Galton and Composite Portraiture."Trans. S. H. Butcher. Web Atomic and Massachusetts Institute of Technology, http://classics.mit.edu/ retrieved November 3, 2012.

[8] Jessica, Taubert. "The composite illusion requires composite face stimuli to be biologically plausible." Vision Research, Vol 49.14 Page(s) 215-220, (2009).

[9] Paulith, Mike. Composite Faces of the World. http://ultrafeel.tv/face-future/ , retrieved

9 December 2012.

[10] Buchala et al. “Global and Feature Based Gender Classification of Faces: A Comparison of Human Performance and Computational Models,”*IEEE Transactions on Pattern Analysis and Machine Intelligence,* Vol 13.5, Page(s) 134-143, (2003).

[11] Baluja et al. “Boosting Sex Identification Performance.” International Journal of Computer Vision Vol 71:1, Page(s) 117-221, (2007).

[12] Michael, Cunningham. "Measuring the physical in physical attractiveness: Quasi-experiments on the sociobiology of female facial beauty." Journal of Personality and Social Psychology, Vol 50:5, Page(s) 112-125, (1986).

[13] Cunningham et al."Their ideas of beauty are, on the whole, the same as ours": Consistency and variability in the cross-cultural perception of female physical attractiveness." Journal of Personality and Social Psychology, Vol 68:2, Pages 112-129, (1995).

[14] Schmidhuber, Jurgen. "Facial Beauty and Fractal Geometry." Istituto Dalle Molle di Studi sull Intelligenza Artificiale Resarch, Pages 35-41, (1998).

[15] CMU Multi-PIE Face Database. Fhttp://www.multipie.org/,retrievedebruary 10, 2013.

[16] Yale Face Database. http://vision.ucsd.edu/content/yale-face-database, retrieved March 19, 2013.

[17] The Facial Recognition Technology (FERET) Database. <http://www.itl.nist.gov /iad/humanid/feret/feret_master.html>, retrieved March 20, 2013.

[18] MIT Centre for Biological and Computational Learning Face Database.

<http://cbcl.mit.edu/software-datasets/FaceData2.html>, retrieved February 20, 2013.

[19] Essex Database. <http://cswww.essex.ac.uk/mv/allfaces/>, retrieved March 10, 2013.

[20] The Extended M2VTS Database. <http://www.ee.surrey.ac.uk/CVSSP/xm2vtsdb/>, retrieved February 18, 2013.

[21] Martinez, Aleix. AR Face Database. <http://www2.ece.ohio-state.edu/~aleix/ARd atabase.html> retrieved February 18, 2013.

[22] BioID Face Database. <http://www.bioid.com/index.php?q=downloads/softwa re/b ioid-face-database.html>, retrived February 18, 2013.

[23] Computational Vision Database. <http://www.vision.caltech.edu/html-files/>, retrieved February 18, 2013.

[24] Langlois et al. "Maxims or Myths of Beauty? A Meta-Analytic and Theoretical Review." Psychological Bulletin 126:3, Pages 110-119, (2000).

[25] Khoo, Charlie. "Perceptions of Beauty in a Western Society." Changing Faces Vol 2, Pages 24-29, (2009).

[26] Posamentier, Alfred. "The Pythagorean Theorem: The Story of Its Power and Beauty." The Mathematical Intelligencer, Vol 34:3, Page(s) 94-116,(2012).

[27] Psychological Image Collection at Stirling. <http://pics.psych.stir.ac.uk/>, retrieved March 12, 2013.

[28] McDonnell et al. "Application of the Golden Ratio to 3D Facial Models." Eurographics Ireland Workshop Pages 56-61, (2003).

[29] Held, Dirk. "Eros, Beauty, and the Divine in Plato." New England Classic Journal 36:3, Pages 12-27, (2009).

[30] Early Theories of Beauty. <http://www2.uiah.fi/projects/metodi/15k.htm>, retrieved April 10, 2013.

[31] Rhodes, Gillian. "The Evolutionary Psyhochology of Facial Beauty." Annual Review Psychology Vol 57, pages 56-71(2006).

[32] Frazier, Christopher. Dynamic Beauty: Cultural Influences and Changing Perceptions-Becoming Prettier or Erasing One's Own Culture? http://hilo.hawaii.edu/academics/hohonu/documents/Vol04x02DynamicBeauty.pdf, retrieved June 14, 2013.

[33] Zeki, Semir. "Art and the Brain." Daedalus, Vol 127:2, Page(s) 45-56, (2000).

[34] Langlois et al. "Facial Diversity and Infant Preferences for Attractive Faces." Developmental Psychology 27:1, Page(s) 123-139, (1991).

[35] Langlois et al. "Attractive Faces are Only Average." Psychological Science Vol 1:2, Page(s) 45-59,(1990).

[36] Miller, Arthur. " A Thing of Beauty." Perspectives, Vol 189:3, Page(s) 89-101,(2006).

[37] Zaidel et al. "Assymetry and Symmetry in the Beauty of Human Faces." Symmetry 2:1, Pages 125-138, (2010).

[38] Zaidel et al. "Appearance of Symmetry, Beauty, and Health in Human Faces." Brain and Cognition 57Pages 135-147,(2005).

[39] Fink et al. "Skin Texture and Color and Attractiveness ." Journal of Comparative Psychology Vol 12, Pages 71-84, (2001).

[40] Chen et al. "A Benchmark of Geometric Facial Beauty Study." Medical Biometrics, Pages 61-65(2010).

[41] FEI Face Database. <http://fei.edu.br/~cet/facedatabase.html>, retrived March 10,

2013.

[42] Indian Face Database. <http://vis-www.cs.umass.edu/~vidit/IndianFaceDatabase/>, retrieved March 10, 2013.

[43] Lopez et al. "Introducing the Golden Section to Computer Science." Proc. of the First IEEE International Conference on Cognitive Informatics (ICCI02), Pages 131-156, 2002.

[44] Farkas et al. "Vertical and Horizontal Proportions of the Face in Young Adult North American Caucasians". Plastic and Reconstructive Surgery Vol 75, Page(s) 92-101, (1985).

[45] T.F Cootes, G.J. Edwards, C.J. Taylor. "Active Appearance Models." Proc. of the European Conference on Computer Vision, Vol. 2 , Page(s) 484-498 (1998).

[46] T.F Cootes, G.J. Edwards, C.J. Taylor. "Active Shape Models-Their Training and Application." Computer Vision and Image Understanding, Vol. 61 , Page(s) 38-59 (1995).

[47] T. F. Cootes, C. J. Taylor, D. H. Cooper, and J. Graham. "Training models of shape from sets of examples". In Proceedings of BMVC'92, Vol. 82 , Page(s) 266–275, (1992).

[48] Michael Spira. "On the Golden Ratio". Proc. of the International Congress on Mathematical Education , Page(s) 23-34, (2012).

[49] L. Farkas & J. Kolar. "Anthropometrics and art in the aesthetics of women's faces". Clinics in Plastic Surgery, Vol. 14: Page(s) 599–616, 1987.

[50] Y. Jefferson. "Facial aesthetics-presentation of an ideal face". Journal of General Orthodontics, Vol 4, Page(s) 18–23, 1993.

[51] B. Finka et al. “Visible skin color distribution plays a role in the perception of age, attractiveness, and health in female faces”. Evolution and Human Behavior, Vol 27, Page(s) 433–442, 2006.

[52] Mihran Tuceryan and Anil K. Jain. “Texture Analysis”. The Handbook of Pattern Recognition and Computer Vision, Page(s) 207-248, World Scientific Publishing Co., 1998.

[53] Dario Valenzano, Andrea Mennucci, Giandonato Tartarelli, Alessandro Cellerino. “Shape Analysis of Female Facial Attractiveness”. Medical Biometrics, Vol 46: Page(s) 1282-1291, 2006.

[54] Wenshuo Gao, Lei Yang, Xiaoguang Zhang, Huizhong Liu. “An Improved Sobel Edge Detection”. IEEE International Conference on Cognitive Informatics (ICCI02), Page(s) 100-115, 2010.

[55] James, David. “Anatomy of the Human Eye”. http://www.ic.uc sc.edu/~bruceb/ps yc123/ Vision1 23.html.pdf, retrieved June 12, 2013.

[56] “Anatomy of Nose and Sinus”. http://ws.ajou.ac.kr/~ ent/knew/education/medical_ stud ent/lecture/ 05_nose_anatomy.pdf, retrieved May 5, 2013.

[57] K. I. Kim, K. Jung, S. H. Park, and H.J Kim, “Support vector machine-based text detection in digital video”, Pattern Recognition, Vol. 34, Page(s) 527-529 (2001).

[58] Muller O'Rahilly, “The mouth, tongue, and teeth.” http://www.dartmouth.edu/ ~humananato my /part_8/cha pter_51.html, retrieved March 9, 2013.

[59] E.Osuna, R.Freund, and F.Girosi, “Training support vector machines: an application to face detection”, Proceedings CVPR'97, Page(s) 56-71, 1997.

[60] C.J.Lin, On the convergence of the decomposition method for support vector

machines, IEEE Transactions on Neural Networks, 12(6), 2001, Page(s) 1288-1298.

[61] T.Joachims, Advances in Kernel Methods: Support Vector Machines , Page(s) 52-71, 1999.